

T H E U N I V E R S I T Y O F M I C H I G A N

COLLEGE OF ENGINEERING
Department of Meteorology and Oceanography

Final Report

WAVE HINDCASTS VS. RECORDED WAVES
Supplement No. 1
(1965 Data)

Alan L. Cole
Associate Research Meteorologist

John C. Ayers
Project Director

ORA Project 06768

under contract with:

U.S. ARMY ENGINEER DISTRICT, LAKE SURVEY
CONTRACT DA-20-064-CIVENG-65-6
DETROIT, MICHIGAN

administered through:

OFFICE OF RESEARCH ADMINISTRATION, ANN ARBOR

May 1967

ensm

UMR0849

TABLE OF CONTENTS

	Page
LIST OF TABLES	
LIST OF FIGURES	
ABSTRACT	
1. INTRODUCTION	1
2. GENERAL CONSIDERATIONS	3
3. WIND ANALYSES	9
4. HINDCAST AND OBSERVED WAVES	15
5. STRONG WIND CONDITIONS	20
6. SUMMARY AND CONCLUSIONS	23
APPENDIX	
A. 1965 WIND DATA AND SCATTER DIAGRAMS FOR MUSKEGON, MICHIGAN	28
B. 1965 WAVE DATA AND SCATTER DIAGRAMS FOR MUSKEGON, MICHIGAN	37
C. 1965 WAVE DATA FOR POINT BETSIE AND PORT HURON, MICHIGAN	63
D. COMPARISON OF 1964 WAVE DATA AT MUSKEGON, MICHIGAN	66
E. SUCCESSIVE APPROXIMATION TECHNIQUE FOR ANALYSIS OF PRESSURE AND WIND FIELDS	70
F. DERIVATION OF THE SIGNIFICANT WAVE HEIGHT AS A FUNCTION OF THE STANDARD DEVIATION	83
BIBLIOGRAPHY	86

LIST OF TABLES

Table	Page	
3-1	Fetches and upwind land stations used in the calculation of Richards winds at the Muskegon tower.	12
4-1	Summary of wind data used with each wave hindcast method.	17
5-1	Summary of wind and wave conditions, 0100E, 29 November 1966. USCGC ACACIA. (44-29.5N 82-53W)	20
6-1	Wind analysis correlation summary.	23
6-2	Significant wave height correlation summary.	24
6-3	Wave period correlation summary.	25
A-1	Surface wind for 1965 wave hindcast period.	29
B-1	Significant wave heights during 1965 hind-cast periods.	38
B-2	Significant period or period of maximum energy for 1965 wave hindcast times.	43
B-3	Period band and maximum wave height for 1965 wave hindcast times.	48
C-1	Significant wave heights and periods for 1965 wave hindcast times. Point Betsie, Michigan.	64
C-2	Significant wave heights and periods for 1965 wave hindcast times. Port Huron, Michigan.	65
D-1	Comparison of SMB, PNJ, PM and OBS wave data for 1964 hindcast periods. Muskegon Research Tower.	67

LIST OF FIGURES

Figure		Page
1-1.	Flow chart of wind and wave analyses.	2
4-1.	Typical wave spectra at Muskegon research tower as produced by the U.S. Army Coastal Engineering Research Center.	19
5-1.	Wind conditions measured by the U.S.C.G.C. ACACIA on 28 November 1966. The base of the arrow indicates the location of the ship while the arrow shows wind direction and speed. The numbers by each arrow are the E.S.T. of the observation.	21
A-1.	Scatter diagram of Bretschneider winds vs. surface (10 meters) measured winds.	34
A-2.	Scatter diagram of the Jacobs 7.5 meter winds vs. surface (7.5 meters) measured winds.	34
A-3.	Scatter diagram of the Jacobs 19.5 meter winds vs. surface (16 meters) measured winds.	35
A-4.	Scatter diagram of the Richards winds vs. surface (16 meters) measured winds.	35
A-5.	Scatter diagram of the Richards winds vs. surface (10 meters) measured winds.	36
B-1.	Scatter diagram of CERC observed significant wave heights vs. those calculated from the standard deviation of the staff gage data.	52
B-2.	Scatter diagram of hindcast significant wave heights calculated by the SMB (Bretschneider winds) method vs. the observed significant wave heights.	52
B-3.	Scatter diagram of hindcast significant wave heights calculated by the PNJ (Jacobs 7.5 meter winds) method vs. the observed significant wave heights.	53

Figure	Page
B-4. Scatter diagram of hindcast significant wave heights calculated by the PM (Jacobs 19.5 meter winds) method vs. the observed significant wave heights.	53
B-5. Scatter diagram of hindcast significant wave heights calculated by the SMB (Richards winds) method vs. the observed significant wave heights.	54
B-6. Scatter diagram of hindcast significant wave heights calculated by the PNJ (Richards winds) method vs. the observed significant wave heights.	54
B-7. Scatter diagram of hindcast significant wave heights calculated by the PM (Richards winds) method vs. the observed significant wave heights.	55
B-8. Scatter diagram of hindcast significant wave heights calculated by the SMB (measured winds) method vs. the observed significant wave heights.	55
B-9. Scatter diagram of hindcast significant wave heights calculated by the PNJ (measured winds) method vs. the observed significant wave heights.	56
B-10. Scatter diagram of hindcast significant wave heights calculated by the PM (measured winds) method vs. the observed significant wave heights.	56
B-11. Scatter diagram of hindcast significant period calculated by the SMB (Bretschneider winds) method vs. the observed period of maximum energy.	57
B-12. Scatter diagram of hindcast period of maximum energy calculated by the PNJ (Jacobs' 7.5 meter winds) method vs. the observed period of maximum energy.	57

Figure		Page
B-13.	Scatter diagram of hindcast period of maximum energy calculated by the PM (Jacobs' 19.5 meter winds) method vs. the observed period of maximum energy.	58
B-14.	Scatter diagram of hindcast significant period calculated by the SMB (Richards' winds) method vs. the observed periods of maximum energy.	58
B-15.	Scatter diagram of hindcast of period of maximum energy calculated by the PNJ (Richards winds) method vs. the observed period of maximum energy.	59
B-16.	Scatter diagram of hindcast of period of maximum energy calculated by the PM (Richards winds) method vs. the observed period of maximum energy.	59
B-17.	Scatter diagram of hindcast significant wave period calculated by the SMB (measured winds) method vs. the observed period of maximum energy.	60
B-18.	Scatter diagram of hindcast wave period of maximum energy calculated by the PNJ (measured winds) method vs. the observed period of maximum energy.	60
B-19.	Scatter diagram of hindcast wave period of maximum energy calculated by the PM (measured winds) method vs. the observed period of maximum energy.	61
B-20.	Frequency distribution of significant wave heights as calculated by the SMB-Bretschneider wind method and the PNJ-Jacobs 7.5 meter wind method and as observed by the staff wave gage.	62

Figure	Page
E-1. The analysis grid and the locations of data sources for the Successive Approximation Technique.	72
E-2. A portion of the Successive Approximation Technique map output.	78
E-3. Computer listing of input pressures for the Successive Approximation Technique analysis.	79
E-4. Gridpoint pressures as calculated by the Successive Approximation Technique.	80
E-5. Contours of the calculated pressure field.	81

ABSTRACT

This study was conducted to evaluate existing methods of wind analysis and wave hindcasting for utilization in the determination of wave climatology for Lakes Huron and Superior. Various calculated and measured winds were used as inputs to the Sverdrup, Munk and Bretschneider (SMB), the Pierson, Newmann and James (PNJ) and the Pierson Moskowitz (PM) wave hindcasting schemes. Of these techniques, the wind analysis of Bretschneider and the SMB wave hindcast method showed better correlations with observed wind and wave data.

The predominant finding of this investigation is that all aspects of wave hindcasting for the Great Lakes are subject to question. Further investigation and development are needed to improve the final product. Despite the preceding statement, the determination of a wave climatology by hindcast methods is feasible at this time.

1. INTRODUCTION

This report is a supplement to the final report of the research program "Wave Hindcasts vs. Recorded Waves", Contract DA-20-064-CIVENG-65-6. The aim of this investigation has been to evaluate wind analyses and wave hindcasting techniques in order to specify the best methods for use in the development of a wave climatology for Lakes Huron and Superior. The original research compared wave hindcasts with measured wave parameters for the intervals from August 1 through August 10 and September 13 through September 23, 1964. The Pierson, Neumann and James, (PNJ) and Pierson and Moskowitz, (PM) wave spectral methods were used to calculate significant wave heights and periods from 1964 data. This supplemental report presents the results of research carried out on 1965 data using the Sverdrup, Munk and Bretschneider (SMB) significant wave height method as well as the PNJ and PM wave spectral techniques.

For the 1965 data, the wave hindcasting was split into three phases. The first phase was a determination of a mesoscale wind field over the lakes while the second phase was the calculation of the surface wind field. Thirdly, with a surface or "anemometer height" wind established, the wave statistics were determined. Figure 1-1 illustrates the combinations of wind analyses and wave hindcast methods that were utilized. The general considerations of the wave hindcast problem are treated in Chapter 2. The wind analyses are discussed in Chapter 3 and the wave hindcasts in Chapter 4. Comparisons made between calculated and observed values of wind and wave parameters are reported in Chapter 6.

The availability of wind and wave measurements from the research tower in Lake Michigan near Muskegon operated by the Great Lakes Division of the University of Michigan determined the dates and times for wave hindcasts during September, October, and November, 1965. In general, these time periods represented growing or fully developed seas.

In addition to the analyses of 1965 data, the SMB method was applied to the 1964 data and results compared with the earlier findings.

In late November, 1966 an intense storm passed over Lake Huron with winds reported to 44 knots and waves to 20 feet. Wind analyses and wave hindcasts were made for the high wind conditions of this storm.

2. GENERAL CONSIDERATIONS

Introduction

The Great Lakes are bodies of water with a maximum dimension of the order of 300 nautical miles embedded in a large continental land mass. Weather and climate of the surrounding land areas are continental with maritime modifications that decrease with distance from the lakes. A true maritime weather or climate does not exist anywhere in the area; however the maritime modification of the continental climate can be very pronounced at times while being minimal at other times. Over the lakes, the atmospheric conditions are normally in a state of transition from the continental character shown over the upwind land areas toward a maritime character over the water. This transition was clearly shown by Richards, Dragert and McIntyre (1966) in their discussion of the variation of the surface wind from a land station to a downwind ship location. They showed that length of overwater fetch and air-sea temperature differences may cause the overwater wind to be as much as three times the land wind. Likewise, Strong and Bellaire (1965) have shown that the reduction of geostrophic winds to surface winds and the heights of Great Lakes waves depend strongly on the stability of the lowest levels of the atmosphere over the lakes. The atmospheric stability has been shown by Bellaire (1965) and Lansing (1965) to have a decided seasonal variation over the lakes. The atmosphere is generally rather stable during the spring and early summer while during the fall and winter it becomes quite unstable. As an unstable atmosphere will transport more momentum downward, the waves should be more energetic in fall and winter. That this is true is easily observed. Likewise, different stability regimes would be expected to produce different wave spectra. No experimental data have been published to show the extent of these variations.

Wave Hindcasts

The direct approach to the problem of determining wave statistics at any location would be to record the wave heights and periods and apply well known statistical methods to the resulting data. However, adequate wave records do not exist and an indirect method of wave hindcasting must be used. By use of wave hindcasting techniques, meteorological records of pressure, wind, temperature, humidity, etc. were analysed to produce a wind field over the bodies of water for which wave statistics were required. From

this field the resultant wave field was determined and the wave statistics calculated. This technique has at least three advantages. First, meteorological records have been kept for many years and many stations in the Great Lakes area as compared with wave records at a few locations and only for limited times. Second, the wave hindcast technique can be applied anywhere on the lakes and especially at locations where the installation of a wave sensor and recorder would be impossible or very costly. Indeed, after the wind field for the Great Lakes area has been calculated, wave statistics can be produced rather rapidly and relatively inexpensively at any new location. Third, with an input of current meteorological data plus a weather forecast the wave hindcast becomes a wave forecast which may be of considerable value to anyone using the lakes for commerce or recreation.

The disadvantages of the wave hindcast method is that it is an indirect method requiring the use of analyses that were developed from ocean data that may not be applicable to the Great Lakes. Indeed the purpose of this investigation was to evaluate these oceanic analytical methods and determine the best one for use on the Great Lakes.

Theoretically, the process of wave hindcasting consists of the following steps:

1. The determination by meteorological methods of a wind field over the water area under consideration.
2. The reduction of the wind field to a wind stress field at the height or heights which are responsible for transferring energy to the wave field.
3. The calculation of the energy transfer from wind field to wave field and the resulting wave lengths, heights and periods as a function of time and location.
4. The computation of the statistics of the wave field.

Of the above four steps, only the first and last have been achieved with any certainty at the present time, and then only with simplifying assumptions, i.e. a geostrophic or gradient wind field can be calculated from the surface pressure field as reduced to sea level. Also, according to Longuet-Higgins (1952), wave height statistics can be calculated if, over a limited frequency range, a Rayleigh distribution can be assumed.

The reduction of the gradient wind field to a wind stress field and its effect on wave generation are areas of micro-meteorology and air-sea interaction that are extremely complicated. Much research effort has been expended on these fields and much more will be required before they become amenable to routine calculations.

In practice, steps 2, 3, and 4 have been combined into semi-empirical relations which generate wave statistics when the wind speed, fetch and duration are known at some prescribed anemometer height. The SMB and PNJ wave hindcasting techniques are examples of these relations.

The investigations conducted for this project were divided into the following three phases:

1. The determination of a meso-scale wind field over the Great Lakes area.
2. The reduction of this wind field to "anemometer height" or "surface winds" over the lakes.
3. The determination of the wave statistics from the speed, fetch and duration of the surface winds.

Phase 1 The Determination of the Meso-Scale Wind Field

A direct determination of the meso-scale wind field by an analysis of streamlines (lines everywhere tangent to the wind vector) and isogons (lines of constant wind speed) from a chart of plotted wind reports often leads to erroneous results, especially for low wind speeds. An anemometer and a wind vane sample the wind only at one point which may be quite non-representative of the actual wind field due to the exposure of the instruments to the wind, i.e. a wind vane located near a river flowing between sand dunes into Lake Michigan will most likely be biased by the channeling effect of the valley. Likewise, the data from anemometers mounted on Great Lakes vessels may well be biased due to the proximity of smoke stacks, wheel houses, and other parts of the superstructure.

Unlike the wind field, the pressure field is a scalar quantity and lends itself to accurate measurement. By use of the geostrophic and/or gradient wind assumptions, a wind field can be computed in a straightforward manner. If there is no change of pressure gradient in the lower atmosphere, an actual wind equal to the gradient wind may be found above the friction layer. However, a vertical change

of horizontal pressure gradient usually exists and the gradient wind is generally a fictitious wind, however, it is one that is reproducible for any given pressure distribution, well known to all meteorologists, and constitutes a convenient and reliable entry into analysis problems such as wave hindcasting.

A program for the IBM 7090 computer has been developed to analyze the pressure field, compute the geostrophic wind, curvature of the isobars, and the gradient wind at grid points spaced 75 km apart over the western Great Lakes area. This objective analysis for the meso-scale wind constitutes a step towards the complete computer program for wave hindcasts that must be perfected eventually.

Phase 2 The Reduction of the Geostrophic or Gradient Wind Field to a Surface Wind.

The geostrophic wind field is calculated from the pressure field under the assumptions that the isobars are straight and parallel, there are no friction forces, and the pressure pattern is invariant with time. The geostrophic wind is thus a result of the balance between pressure gradient and Coriolis forces. The gradient wind is similar except the isobars are assumed to be circular and the wind is the resultant motion due to a balance of pressure gradient, Coriolis and centrifugal forces. In the boundary layer near the surface of the Earth these assumptions are never fully satisfied and rarely approached. Indeed, the exact detailed solution of the problem with friction, randomly curved and spaced isobars, energy and humidity exchanges, time dependence of all variables and parameters, etc. is an extremely difficult if not impossible task. The lack of requisite data is a prime reason for relatively little progress in this field. Therefore, the common practice is to calculate the geostrophic or gradient wind and determine, empirically, the deviations of speed and direction at or near the surface. These deviations have been studied as functions of atmospheric stability, isobaric curvature, overwater fetch, etc.

Bretschneider (1952) published a surface wind chart showing the ratio between the surface wind (defined as 10 meters above the mean sea surface) and the geostrophic wind vs. the difference in sea-air temperature ($T_s - T_a$) for various radii of cyclonic and anti-cyclonic curvature. The chart was based on oceanic data originally obtained by Arthur (1947).

Richards, Dragert and McIntyre (1966) have reported on the influence of atmospheric stability and length of overwater fetch on

the ratio U_w/U_1 where U_w is the wind as measured on a vessel on Lake Erie or Lake Ontario^w and U_1 is the wind speed at an upwind land station. This report showed the lake winds to be greater than the land winds except under very stable conditions. They also showed that under unstable over-lake conditions the wind increased with fetch up to a fetch of about 25 nautical miles, but no further increase occurred with additional fetch. They did not consider geostrophic or gradient winds and did not display equations for calculating surface lake winds. This method of calculating winds has been tested with the SMB, PNJ, and PM wave hindcasting methods.

Strong and Bellaire (1965) published data on the effect of air stability, as measured by the air-lake temperature difference, on wind and waves for Lake Michigan. This report included regression equations for the computation of surface winds from geostrophic winds. These findings were based on ship observations of wave height, which are estimates only and on ship reports of winds, which are sometimes biased by the location of the wind sensors. However, these data and the equations derived from them by Jacobs (1965) constitute an available technique for reducing gradient wind speed to surface wind speed for the Great Lakes and they were used for computing winds for the PNJ wave hindcasting method.

Phase 3 The Determination of the Wave Statistics From Surface Winds.

The term wave statistics is used in a broad sense and includes any result of statistical manipulations of wave height data. Under this definition, wave spectra are wave statistics as are such obvious quantities as mean wave height, significant wave height, etc. The wave statistics produced by this investigation are the significant wave height and the significant wave period.

The field of ocean wave spectra and wave statistics is an active research area in which the theories of Bretschneider and associates and Pierson-Neumann and associates predominate with Darbyshire, Longuet-Higgins, Wilson and others making significant contributions. There has been no agreement as to which of the wave spectra forms advocated by these leaders in the field will best describe ocean-wave fields. However, recent, Pierson (1965), publications indicate their results may be approaching each other as they better define such quantities as "the anemometer height wind". The SMB, PNJ and PM methods were evaluated in this study and the SMB found to correlate best with measured wave data.

Observed Winds and Waves

Wind and wave values, for comparison with those calculated from the various schemes, were obtained from the data taken at the research tower in Lake Michigan near Muskegon, Michigan. This tower, operated by the Great Lakes Division of the Institute of Science and Technology of the University of Michigan extended 16 meters above the water and was located approximately one mile from the shore. An Aerovane wind speed and direction sensor was mounted at the top and Climet 3-cup anemometers and resistance thermometers were installed on the tower to provide wind profile and lapse rate data. Thermometers in the water measured water temperature and a staff gage on the tower gave wave data. Humidity measurements were also taken.

When these instruments and their recorders were operational, they provided the data for comparison and evaluation with the calculated parameters. However, failures did occur and all desired data were not available at all times.

3. WIND ANALYSES

Introduction

One of the major factors in any wave hindcasting method and often one of the greatest causes of error is the calculation of the wind field responsible for the wave development. The problems of wind field analysis may be conveniently divided into two categories. First, there is no agreement among authorities in the field as to what wind should be determined and secondly, the methods of obtaining the desired wind or wind profile or wind spectra are not well understood. This report will not treat the first problem as the input wind requirements for each wave hindcasting scheme have been accepted as published. Methods of obtaining mean winds at various specified heights of the atmosphere have been evaluated by comparing calculated winds with measured winds at the Muskegon research tower.

Bretschneider Wind

The name "Bretschneider Wind" has been applied to the wind input for the SMB wave hindcasting method as outlined by the U.S. Army Corps of Engineers (1961). A surface wind scale, Bretschneider (1951), relates the sea-air temperature difference to the ratio of surface wind vs. geostrophic wind for a family of curves of varying cyclonic and anticyclonic curvature. From the surface wind vs. geostrophic wind ratio and the geostrophic wind the surface wind was easily calculated.

The data used to determine the sea-air temperature difference came from a number of sources. Lake temperatures were obtained from the water temperature measurements at the Muskegon research tower and the instrumented ships on the Great Lakes. Air temperatures came from the above sources and from U.S. Weather Bureau reports at land stations near the lake. Continuity and extrapolation were widely employed to arrive at a best estimate of the temperatures in the wave generating area. The lake-air temperature data are poor but probably contain no greater error than other aspects of the wave hindcast procedures. There is no account taken of the spatial variability of surface temperature and none can be expected in the near future due to a serious lack of measurements.

The geostrophic wind speeds and the radii of curvature of the streamlines were obtained from weather maps using a geostrophic wind scale and a curvature scale. The weather maps, obtained from the Chicago forecast center of the U.S.W.B., were reanalyzed for 1 mb isobars in the vicinity of Lake Michigan prior to the calculation of geostrophic wind speed and curvature. The calculated wind direction was taken to be the direction of the isobar located nearest to Muskegon, Michigan.

The calculated Bretschneider winds for the 1965 data are listed in Table A-1 of Appendix A and should be compared with the 10 meter observed winds at the Muskegon tower listed in the same table. Figure A-1 is a scatter diagram of the Bretschneider winds vs. the observed 10 meter winds. The correlation coefficient of 0.63 between the Bretschneider winds and the observed winds was the best obtained for any calculated wind.

Jacobs 7.5 meter winds

For the PNJ wave hindcast scheme, Jacobs (1965) presented the following empirical equations for the calculation of the surface (7.5 meters) wind from the gradient wind.

$$\begin{aligned}
 V &= \text{wind speed at 7.5 meters in knots} \\
 &= 7.9 + .28 V_g & \Delta T < -5^\circ\text{F} & \text{Stable} & (3-1) \\
 &= 9.5 + .27 V_g & -5^\circ\text{F} \leq \Delta T \leq 5^\circ\text{F} & \text{Neutral} & (3-2) \\
 &= 13.1 + .31 V_g & \Delta T > 5^\circ\text{F} & \text{Unstable} & (3-3)
 \end{aligned}$$

where V_g is the gradient wind calculated from surface pressure data and ΔT^g is the water-air temperature difference, i.e. a stability factor.

The gradient wind, V_g , was calculated by the standard meteorological equations:

$$V_g = \frac{f\rho}{2} - \sqrt{\frac{f^2\rho^2}{4} - f\rho V_{geo}} \quad \text{for anticyclonic curvature} \quad (3-4)$$

$$V_g = -\frac{f\rho}{2} + \sqrt{\frac{f^2\rho^2}{4} + f\rho V_{geo}} \quad \text{for cyclonic curvature} \quad (3-5)$$

where V_{geo} = the geostrophic wind in knots,

ρ = radius of curvature of isobar lines in nautical miles

f = Coriolis parameter

The results of these calculations are shown in Table A-1. The corresponding measured winds, for comparison, are listed under the heading of Muskegon Tower 7.5 meter winds. Figure A-2, a scatter diagram of the Jacobs 7.5 meter winds vs. the measured 7.5 meter winds shows the calculated winds to be generally larger than the measured winds. The linear correlation coefficient between these winds was 0.56.

Jacobs 19.5 meter winds

Wave statistics as determined from the Pierson-Moskowitz spectrum require a mean wind input for 19.5 meters. Jacobs (1965) developed ratios between the 7.5 and 19.5 meter winds as measured in 1963 and 1964 on the Muskegon tower (Elder, 1965).

$$\frac{V}{U} = \frac{\text{wind speed at 7.5 m}}{\text{wind speed at 19.5 m}}$$

$$= .85 \quad \Delta T < -5^\circ\text{F} \quad (3-6)$$

$$= .95 \quad -5^\circ\text{F} \leq \Delta T \leq +5^\circ\text{F} \quad (3-7)$$

$$= 1.00 \quad \Delta T > 5^\circ\text{F} \quad (3-8)$$

These ratios were used with the Jacobs 7.5 meter winds to obtain the Jacobs 19.5 meter winds which are listed in Table A-1. The Muskegon tower was 16 meters high with an Aerovane wind speed and direction sensor on top. The data from the Aerovane system was used to compare with the Jacobs 19.5 meter wind as illustrated by the scatter diagram, Figure A-3. The wide scatter of these data is obvious and is confirmed by the low correlation coefficient of 0.27.

Richards Winds

In the Monthly Weather Review, Richards, Dragert and McIntyre (1965) reported ratios of overwater wind to overland wind as functions of the atmospheric stability and the fetch from land to the overwater wind observation location. They used ship winds and water temperatures with upwind land station winds and air temperatures to calculate the ratios of overwater wind to overland wind. These ratios were then tabulated according to fetch and the stability parameter, $T_a - T_w$.

These ratios were used to calculate an overwater wind at the Muskegon tower using the Muskegon tower water temperature and an upwind land-station air temperature and wind speed. The upwind land-stations were chosen on the basis of the wind direction at the Muskegon tower or the Muskegon U.S.W.B. The wind directions considered, their fetches and the upwind land stations used are listed in Table 3-1 below:

Table 3-1

Fetches and upwind land stations used in the calculation of Richards winds at the Muskegon tower.

<u>Wind Direction</u>	<u>Overwater fetch n mi.</u>	<u>Upwind Land Station</u>
180°	50	5/3 St. Joseph, Mich.
190°	80	SBN South Bend, Ind.
200°	98	SBN
210°	102	ORD O'Hare Airport Chicago, Ill.
220°	91	ORD
230°	86	ORD
240°	77	MKE, 53/ Milwaukee, Wis.
250°	68	MKE, 53/

<u>Wind Direction</u>	<u>Overwater fetch n mi.</u>	<u>Upwind Land Station</u>
260 ^o	69	MKE, 53/ Milwaukee, Wis.
270 ^o	70	MKE, 53/
280 ^o	69	MKE, 53/
290 ^o	68	MKE, 53/
300 ^o	71	GRB, MTW, Green Bay or Manitowac, Wis.
310 ^o	79	GRB, MTW
320 ^o	84	GRB, MTW
330 ^o	100	GRB, MTW

The Richards winds data are tabulated in Table A-1 and compared with the Aerovane winds from the Muskegon tower on the scatter diagram, Figure A-4. These data show the calculated winds to be generally lower than the corresponding Aerovane measured winds.

When compared with the 10 meter Muskegon tower winds, Figure A-5, the Richards winds are seen to scatter rather widely but have no particular trend with respect to the observed winds.

The concept of determining the overwater wind by the technique used above seems very sound from a conceptual view; however, practical considerations appear to make it not acceptable. The major sources of error probably are due to the strong dependence of the method on the value of the upwind land station winds and the stability factor over the lake. The latter are not measured with any regularity and the former suffer from being non-representative short time averages at single locations. Jacobs (1965) showed that the Muskegon U.S.W.B. wind speed data correlated poorly with either Muskegon tower winds or with ship winds.

Wind Direction

The only calculated wind directions were obtained by assuming that the geostrophic and gradient winds have the same direction as the isobars from which they were derived. These wind direction data are listed in Table A-1 with the corresponding wind directions as measured by the Aerovane instrument on the Muskegon tower. As predicted by the theory and observations, the measured wind shows a tendency to flow across the isobars toward lower pressure. A mean deviation

of 29° from the isobaric direction was calculated from the data. There is nothing new or unusual about these findings. They merely verify accepted data and hypotheses.

Successive Approximation Technique

The successive approximation technique of Cressman (1959) has been applied to a pressure analysis of the Great Lakes area. From the pressure analysis, geostrophic and gradient wind can be computed. While the technique is described in detail in Appendix E, it is pertinent at this point to mention that it is a computer analysis technique that produces a smoothed pressure and geostrophic wind analysis. The smoothing built into this program should make the results more representative of the wind over an area the size of Lake Michigan and therefore better wave hindcasts should result.

Discussion and Recommendations

The Bretschneider winds correlated with the observed wind better than any other wind analysis technique. However, a correlation coefficient of 0.63 for 36 pairs of data is not a high correlation. It is apparent that additional knowledge of the lower level wind systems must be obtained before improved accuracy in wave hindcasting can be achieved. The successive approximation technique should be the first step in an improved analysis method. From the calculated pressure field, geostrophic wind field, or gradient wind field, a surface wind must be calculated taking into account the overwater stability, the upper air stability, fetch, wind speed, etc. Indeed, according to Pierson (1964) and Harris, (1967) the measurement of a mean wind at one level provides insufficient data for the determination of surface stress and wave spectra. Thus the more difficult problem of calculating the surface stress or wind profiles from the synoptically observed data has been posed. Progress along these lines will not be quick and it appears the best procedure at this time is to compute the geostrophic wind which can be reduced to a lake level (10 meters) wind by Bretschneider's surface wind speed curves. Research should continue to upgrade these procedures.

4. HINDCAST AND OBSERVED WAVES

Introduction

Two wave hindcasting methods have achieved prominence in the United States. These are the Sverdrup, Munk and Bretschneider, (SMB) method and the Pierson, Neumann and James (PNJ) method. Both methods are applicable to fetch and duration limited seas as well as fully developed seas and both are semi-empirical as experimental data was used in some phase of their derivations. The SMB method predicts two statistics of the wave field: the significant wave height and the significant wave period. From these two statistics wave spectra and other statistics can be calculated using the wave distribution of Longuet-Higgins (1952). The PNJ method predicts the wave spectra, from which wave statistics can be computed by use of the wave distribution of Longuet-Higgins (1952). In recent years the wave spectra and wave statistics derived from both methods have become more nearly equal.

A third hindcast method, the PM method, due to Pierson and Moskowitz (1964) is very similar to the PNJ method except that a different spectra is calculated from the input data. However, no procedure has been published for wave spectra calculations when fetch and duration are limited. This limitation seriously curtails the usefulness of the method for Great Lakes wave hindcasting.

The SMB Wave Hindcast Method

The SMB method originated with Sverdrup and Munk's (1947) consideration of the transfer of energy from the wind field to the wave by both normal and tangential stresses. They assumed the energy of the wave field would increase until an equilibrium condition was reached where the rate of energy transfer from the wind to the waves equalled the rate of energy dissipation from the waves. This condition was called the fully developed sea and was characterized by a condition of maximum wave heights, periods, and speeds for a given wind speed. The fully developed sea is also independent of fetch and wind duration. The theoretical work of Sverdrup and Munk required knowledge of coefficients and constants that could be determined only from empirical data, which at the time were rather meager. With additional data, Bretschneider (1951 and 1958) revised the forecasting relations of Sverdrup and Munk (1947) into the SMB method.

From these relations a series of deep water wave forecasting curves were developed which now appear in many reports and books; U.S. Army Corps of Engineers (1961) and Bretschneider (1965).

The SMB wave forecasting (hindcasting) method requires the following input parameters:

- a. The surface (10 meters) wind speed.
- b. The duration of the wind from the given direction.
- c. The overwater fetch.

With these wind parameters and the SMB wave hindcasting curves, the wave parameters of significant wave height and significant wave period can be obtained. The significant wave height is defined as the average of the highest 1/3 of the wave heights of a given wave train of at least 100 consecutive waves, while the significant wave period is the average period of these same waves. Bretschneider (1965) pointed out that the significant wave period is also a period around which is concentrated the maximum wave energy. This latter concept allows the SMB significant wave period to be compared with the period of maximum energy as determined from measured wave data. Longuet-Higgins' (1952) presentation of the Rayleigh distribution for wave height variability based on a narrow spectrum and its subsequent verification by Bretschneider (1957 and 1959) and others permits many statistical parameters to be determined from the significant wave height. Bretschneider (1965) has reviewed the state of the art of wave generation in general and the SMB method in particular; therefore, the method will be discussed no further except as it relates directly to the problem of Great Lakes wave hindcasting.

The PNJ Wave Hindcast Method

The PNJ wave hindcasting method is attributed to Pierson, Neumann and James (1955) and is a development of Neumann's (1952) theoretical wave spectrum of energy. The PNJ method predicts an E-value, where E is related to the generated wave energy; from which, by use of the theoretical wave distribution of Longuet-Higgins (1952), wave statistics can be calculated. In particular, the significant wave height, the period of maximum energy, the average wave height, and the upper period and lower period for significant wave energy were calculated. Jacobs (1965) has discussed the PNJ method in considerable detail, as have other authors, hence it will not be reviewed further except when pertinent to Great Lakes wave hindcasting.

The input data for the PNJ method are listed below:

- a. Average surface (7.5 meter) wind speed.
- b. Duration of surface wind from given direction.
- c. Fetch of surface wind.

It will be noted that these parameters are the same as those for the SMB method except the surface wind is specified to be at 7.5 meters rather than 10 meters.

The Pierson-Moskowitz Spectrum

For a fully developed sea, Pierson and Moskowitz (1964) proposed a wave spectrum based on the similarity theory of Kitaigorodski (1961). Jacobs (1965) has reviewed this spectrum and tabulated the equations used to calculate appropriate wave statistics. However, the requirement of a fully developed sea severely restricts the application of this spectrum to the wave hindcasting problem.

The Calculated Wave Statistics

Wave statistics were determined using the SMB, PNJ, and PM methods with calculated and measured wind inputs. Table 4-1 summarizes the input wind data used with each wave hindcast method.

Table 4-1

Summary of wind data used with each wave hindcast method.

<u>Wave Hindcast Method</u>	<u>Input Wind Data</u>
SMB	1. Bretschneider Wind 2. Richards Wind 3. 10 meter Measured Wind
PNJ	1. Jacobs 7.5 meter Wind 2. Richards Wind 3. 7.5 meter Measured Wind
PM	1. Jacobs 19.5 meter Wind 2. Richards Wind 3. 16 meter Measured Wind

The significant wave height and the significant wave period or period of maximum energy were calculated for each of these cases and compared with measured significant wave heights and periods of maximum energy. In addition, the period band, within which resides 92% of the wave energy, was calculated from the PNJ method using the Jacobs 7.5 meter wind.

Observed Wave Statistics

The U.S. Lake Survey operated a staff wave-gage on the Muskegon tower during the 1965 wave hindcast periods. Data from this gage were used to calculate the observed significant wave height and period of maximum energy during the hindcast periods. These calculated heights and periods were used as the standard or "correct" value for comparison with hindcast heights and periods.

Staff-gage data for the selected wave hindcast periods of 1965 were analyzed by the U.S. Army Coastal Engineering Research Center using their wave spectrum analyzer, Caldwell and Williams (1961). The wave analyzer output, Figure 4-1, is a spectral curve of the frequency distribution of the linear average and square average wave heights taken over a twenty minute time interval with a filter band width of 0.027 cycles per second. In addition, the cumulative peak wave height is displayed. The period of maximum energy is read directly from the spectrum as the abscissa of the maximum value of the square average wave height curve. The significant wave height for a spectrum is readily obtained from the relation:

Significant Wave Height = $\frac{\text{Maximum Linear Average Value}}{0.45}$
due to Caldwell (1963).

The significant wave height can also be obtained by calculating the standard deviation of the staff-gage data and multiplying by four. This relation is derived in Appendix F. The standard deviation was computed as a running mean of the preceeding twenty minutes of real-time staff-gage record using the hybrid analog/digital computer of the Department of Meteorology and Oceanography, University of Michigan.

The significant wave heights as computed by the standard deviation method and the periods of maximum energy as read from the spectral curves constituted the check data for evaluation of the wave hindcasts.

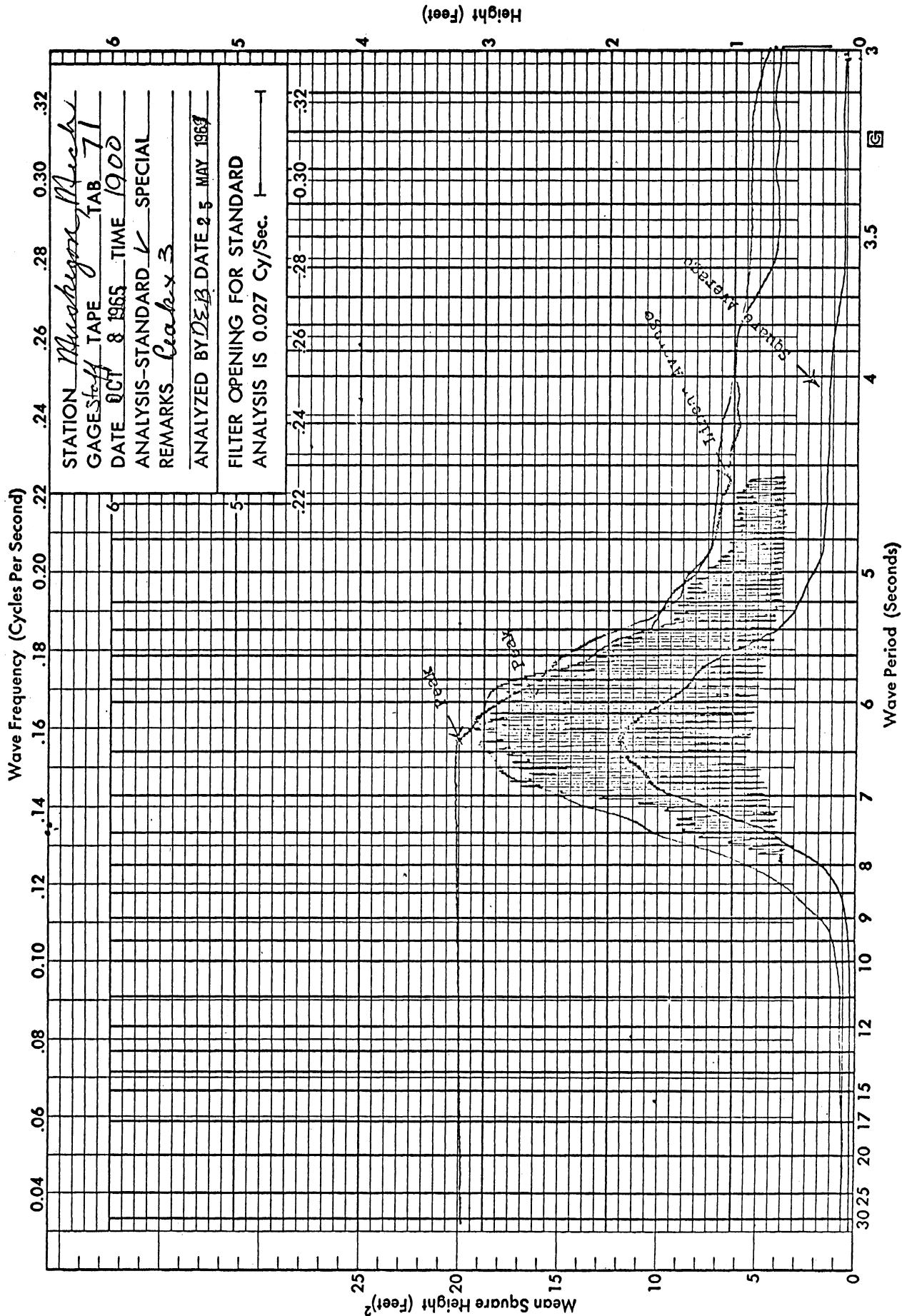


Figure 4-1. Typical wave spectra at Muskegon research tower as produced by the U.S. Army Coastal Engineering Research Center.

5. STRONG WIND CONDITIONS

A sizeable fraction of the wave hindcasts of this study were made for wind speeds, in knots, ranging from the low teens to the high twenties. Indeed, 28 knots was the highest observed wind speed of all the 1965 data. However, wave destruction on the Great Lakes is usually caused by winds that exceed 28 knots. One opportunity for study of a strong wind situation occurred during late November, 1966 when a low pressure system deepened over northern Lake Huron and produced abnormally high winds and waves. On the 28th. of November the U.S.C.G.C. ACACIA ventured into southern Lake Huron and recorded winds to 44 knots and waves estimated to 20 feet. Figure 5-1 shows her location and the measured wind at various times. Wind analyses and wave hindcasts were made for 0100E on 29 November 1966 when the ACACIA was well into Lake Huron and the wind and waves were near their maximum values. The results of these analyses are listed below:

Table 5-1

SUMMARY OF WIND AND WAVE CONDITIONS
0100E 29 NOVEMBER 1966
U.S.C.G.C. ACACIA (44-29.5 N 82-53 W)

	Winds (kts.)	Significant Wave Height (ft.)	Wave Period
SMB- Bretschneider Winds	68		
PNJ- Jacobs 7.5 meter Winds	25		
Richards Winds	28-46		
Bretschneider- Jacobs Average Winds	47		
SMB- Bretschneider-Jacobs Average Winds		19	10.3
PNJ- Bretschneider-Jacobs Average Winds		14	8.1
USCGC ACACIA	42	20	

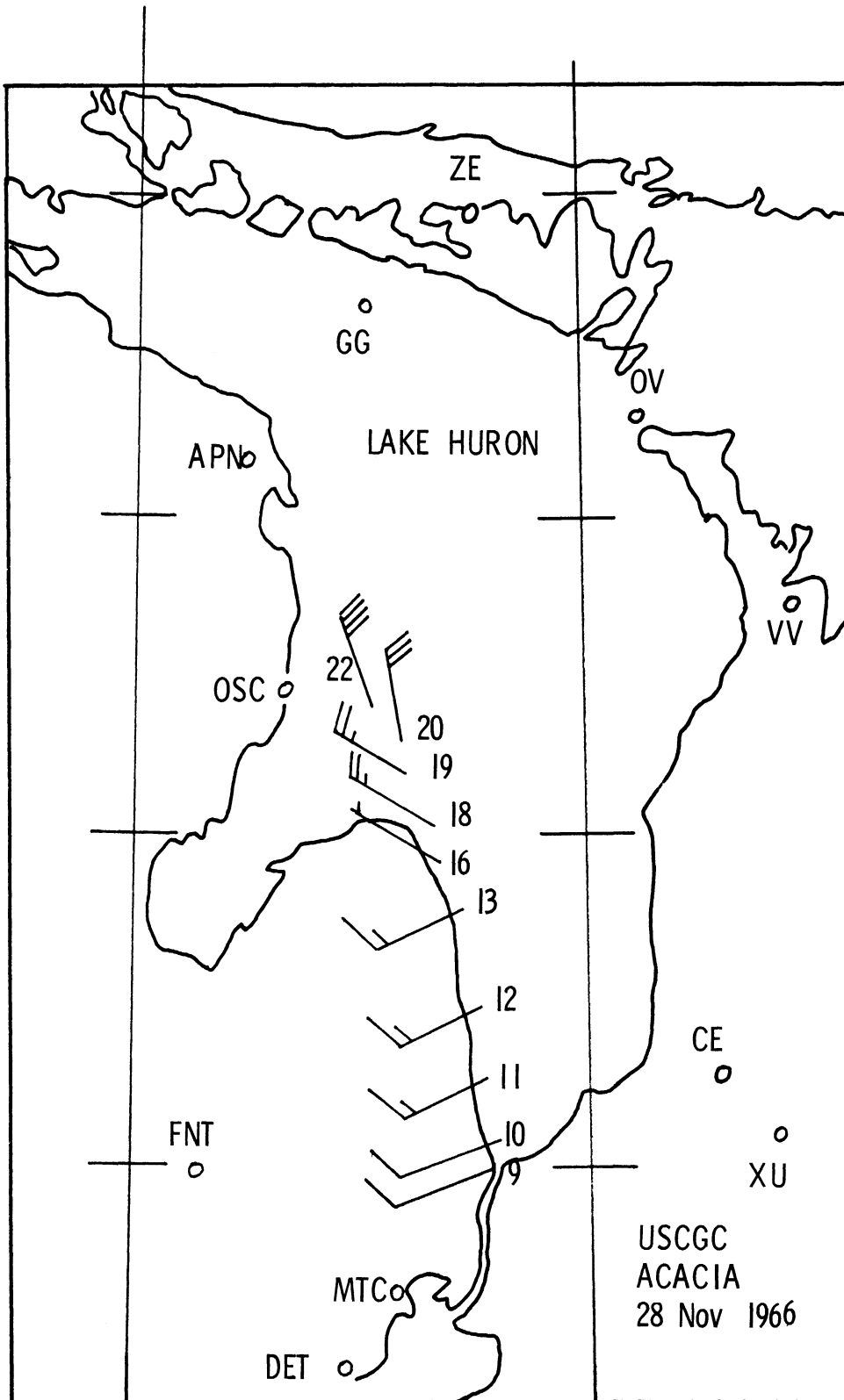


Figure 5-1. Wind conditions measured by the U.S.C.G. C. Acacia on 28 November 1966. The base of the arrow indicates the location of the ship while the arrow shows wind direction and speed. The numbers by each arrow are the E.S.T. of the observation.

After calculating the Bretschneider wind to be 68 knots and the Jacobs 7.5 meter wind to be 25 knots it became apparent that both schemes were badly in error. With a strong wind and extremely unstable atmosphere conditions, $T_{\text{Lake}} - T_{\text{air}} = +8^{\circ}$ to $+18^{\circ}\text{F}$, there should be very little difference between a 10 meter wind speed and a 7.5 meter wind speed. Therefore, averages of the Bretschneider winds and Jacobs 7.5 meter winds were calculated and used for wave hindcasting. This average of 47 knots for 0100E on 29 November 1966 compares favorably with the ACACIA's measured wind of 42 knots. The Richards wind of 38 to 46 knots very nicely bracketed the 42 knot observed wind. Using the average winds with the SMB and PNJ wave hindcast methods, significant wave heights of 19 and 14 feet, respectively, were obtained. The estimate of 20 foot wave heights from the ACACIA compares well with the SMB significant wave height of 19 feet.

This exercise in wave hindcasting for strong wind conditions points out inadequacies in the wind analysis schemes. Possibly these techniques were developed from data biased toward lower wind conditions and do not extrapolate well to stronger winds. It appears that investigations into high wind conditions are required in order to accomplish further improvements in the wind analyses and wave hindcast procedures.

6. SUMMARY AND CONCLUSIONS

Summary of results

Tables A-1, B-1, and B-2 of Appendices A and B tabulate all observed and hindcast values of the surface wind, the significant wave heights and the significant wave periods, respectively for the 1965 data at the Muskegon research tower. Figures A-1 through A-5 of Appendix A and Figures B-1 through B-19 of Appendix B are scatter diagrams of calculated vs. observed values of winds, significant wave heights, and significant wave periods. On each scatter diagram, the line of perfect correlation (45° line) has been drawn as well as the least-squares regression line. The regression equation for the plotted data and the correlation coefficient are also displayed on each scatter diagram.

Figure B-20 is a frequency distribution of significant wave heights for the SMB-Bretschneider wind method, the PNJ-Jacobs 7.5 meter wind method and the observed values. These curves show a similar gross behavior. However, a chi square test indicated that the hypothesis that the SMB and PNJ data were drawn from the same set of random variables as the observed data must be rejected at the 99.5% significance level.

Table 6-1, a summary of the correlation coefficients between calculated and measured wind speeds, shows how the Bretschneider winds correlated better with measured winds than did the other analyzed winds. The 10 meter, 7.5 meter and 16 meter winds used for comparison were those measured on the Muskegon research tower.

Table 6-1

WIND ANALYSES CORRELATION SUMMARY

	<u>n</u>	<u>r</u>
Bretschneider Winds vs. 10 meter winds	36	.63
Jacobs 7.5 meter winds vs. 7.5 meter winds	43	.55
Jacobs 19.5 meter winds vs. 16 meter winds	49	.37
Richards winds vs. 16 meter winds	44	.36
Richards winds vs. 10 meter winds	36	.24

n = number of data pairs
r = correlation coefficient

Table 6-2 summarizes the significant wave height results of this research and clearly shows how the SMB wave hindcast values correlate better than either the PNJ or the PM. It should be noted that the SMB method correlates best with measured wind input as well as with the calculated Bretschneider wind input. In all cases, the significant wave height listed was correlated with that obtained from the standard deviation calculation, Appendix F. The CERC observed significant wave heights were calculated from the CERC wave spectra.

Table 6-2

SIGNIFICANT WAVE HEIGHT CORRELATION SUMMARY

	<u>n</u>	<u>r</u>
CERC observed significant wave heights	85	.89
SMB-Bretschneider Wind	69	.60
PNJ-Jacobs 7.5 meter wind	73	.35
PM-Jacobs 19.5 meter wind	30	.32
SMB-Richards wind	59	.36
PNJ-Richards wind	74	.46
PM -Richards wind	36	.15
SMB-Measured wind	53	.62
PNJ-Measured wind	37	.47
PM-Measured wind	16	.34

n = number of data pairs
r = correlation coefficient

Table 6-3 summarizes the wave-period correlation coefficients obtained by comparing hindcast values with those measured by the CERC spectrum analysis. With the Richards wind input and with the measured wind input, the SMB method showed a higher correlation of wave periods than did PNJ or PM. However, PM with Jacobs 19.5 meter wind input correlated better than SMB with Bretschneider wind input or PNJ with Jacobs 7.5 meter wind input.

The latter three correlation coefficients are all so small that none of these techniques can be designated as a reliable method.

Table 6-3

WAVE PERIOD CORRELATION SUMMARY

	<u>n</u>	<u>r</u>
SMB-Bretschneider Winds	68	.20
PNJ-Jacobs 7.5 meter winds	72	.11
PM-Jacobs 19.5 meter winds	31	.31
SMB-Richards winds	50	.40
PNJ-Richards winds	54	.37
PM -Richards winds	32	.17
SMB-Measured 10 meter winds	51	.67
PNJ-Measured 7.5 meter winds	31	.51
PM-Measured 16 meter winds	13	.64

n = number of data pairs

r = correlation coefficient

Table C-1 of Appendix C lists significant wave heights and periods calculated for Point Betsie, Michigan during some of the time intervals studied at Muskegon. As comparative observed values were not readily available these data do not contribute to the evaluation of wind analysis and wave hindcasting techniques for the Great Lakes.

Table C-2 lists significant wave heights and periods for Port Huron, Michigan during the same times. As the Muskegon data were selected for onshore winds on the eastern shore of Lake Michigan, most days considered showed offshore winds at Port Huron and drastically short fetches. Therefore, these data are very limited and of no value in the evaluation.

Table D-1 of Appendix D compares significant wave heights and periods for the days in 1964 that were previously considered by Jacobs. The PNJ, PM, and OBS values are repeated from Jacobs (1965) report while the SMB values are new. The wind speed and fetches were too low for an SMB analysis in many cases, so the points that can be compared are rather limited. Perusal of these data does not point out any marked superiority of any technique.

Conclusion

The results of this investigation show the Bretschneider wind analysis method produced the best surface mean winds and the SMB wave hindcast method calculated the best significant wave heights. The latter result is undoubtedly due in part to the better fit of the Bretschneider winds to the measured winds. However, the SMB method also produced better wave hindcasts when measured winds were used as input to the hindcast schemes, thus the combination of Bretschneider winds and SMB wave hindcasts appears to be the best method to be utilized, at this time, for wave statistics studies on the Great Lakes.

Despite being the best method available, neither the Bretschneider wind correlation coefficient of 0.63 nor the SMB Bretschneider significant-wave correlation coefficient of 0.60 are outstanding. The SMB-Bretschneider wave-period correlation coefficient of .20 is an indication that wave periods on the Great Lakes can not be hindcast with any accuracy. Indeed, a coefficient of .20 indicates almost a lack of correlation; a fact that is born out by the scatter diagram, Figure B-11.

Both the wind analysis and the wave hindcasting methods are not totally adequate and research in both fields must continue in order to improve the existing methods or develop new ones. However, more data will be necessary before significant advances can be expected.

The results of the investigation of the November, 1966 storm indicate the wind analysis schemes are biased toward low wind speed data. Indeed, the Jacobs wind equations were derived with data containing very few wind speeds greater than 30 knots. While the results of one study of one storm compared with the observations from one ship can not refute existing wind analysis and wave hindcast techniques, these results do raise questions as to the applicability of these techniques to high wind conditions. As the high wind conditions are the most important for any user of a wave climatology, it is imperative that they be studied in greater detail.

Wave Climatology for Lakes Huron and Superior

The production of a wave climatology for the Great Lakes should proceed at this time using the following procedure:

1. With synoptic weather data (0000, 0600, 1200, 1800 GCT), use the successive approximation technique machine-analysis to calculate a surface pressure field and a geostrophic wind field. All output data should be stored on computer tape for future input to newly developed programs.
2. Determine a stability factor, $T_{\text{water}} - T_{\text{air}}$ from a subjective analysis of water temperature climatology, ship records, etc. Continuity, smoothing, interpolation and extrapolation must be judiciously applied to this process. Measure isobaric curvature on a weather chart.
- 3a. Use the Bretschneider surface wind chart with the stability factor and the isobaric curvature to determine the ratio of surface-wind to geostrophic-wind. Calculate the surface (10 meter) wind field upwind of each wave hindcast location.
- 3b. If the calculated surface wind exceeds 30 knots, Jacobs empirical wind equations and the Richards, Dragert and McIntyre computations should be utilized to obtain additional wind estimates. These must be considered, along with ship and land wind reports, in the final determination of surface wind speed.
4. Use the SMB wave hindcast charts to determine the significant wave height and significant wave period.
5. For high wind or fast moving storm conditions, reduce the time between analyses from 6 hours to 3 hours.

The wind analysis and wave hindcast schemes discussed in this report and proposed above for the development of a wave climatology should be considered to be the best available now but improvements in the future are vitally needed and must be anticipated. The program of wave climatology production must remain flexible so that any new developments can be rapidly exploited.

APPENDIX A

1965 WIND DATA AND SCATTER
DIAGRAMS FOR MUSKEGON, MICHIGAN

TABLE A - 1

SURFACE WIND FOR 1965 WAVE HINDCAST PERIOD

Muskegon Research Tower

- V_g = Geostrophic Wind
- V_{gr} = Gradient Wind
- V_R = Richards Wind
- V_{J_2} = Jacobs Wind (19.5 meters)
- V_B = Bretschneider Wind (10 meters)
- V_{J_1} = Jacobs Wind (7.5 meters)

Date:Time(C.S.T.)	<u>Wind Speed (kts)</u>							<u>Wind Direction</u> (degrees)					
	Observed	16m	10m	7.5m	V_g	V_{gr}	V_R		Calculated	V_{J_2}	V_B	V_{J_1}	Observed
September, 1965													
23:0000	15	16	14.6	25	25	15	17	17	16	17	17	240	260
23:0600	12		17	33	31	11	19	19	22	19	19	230	260
23:1200	24	22	24	28	28	16	22	22	20	22	22	210	250
23:1800	20	19	20	30	30	19	22	22	19	22	22	260	310
24:0000	14	12	13	25	25	16	21	21	17	21	21	290	290
24:0600	16	14	15	23	18	13	19	19	16	19	19	290	310
24:1200	17	14	15	25	28	15	22	22	21	22	22	280	310
24:1800	18	16	16	28	35	11	24	24	25	24	24	260	290
25:0000	20	18	18	35	35	13	24	24	26	24	24	260	270
25:0600	22	20	20	48	39	17	25	25	33	25	25	240	270
25:1200	24	21	20	35	61	18	32	32	29	32	32	210	250
25:1800	22	18	18	16	17	19	15	15	10	15	15	200	240
26:0000	11	11	11	0	0	22	0	0	0	0	0		
26:0600	20	13	12	35	26		21	21	23	21	21	cont'd	

Wind Speed (kts)

Date:Time (C.S.T.)	<u>Observed</u>			<u>Calculated</u>					<u>Wind Direction</u> (degrees)		
	16m	10m	7.5m	V _g	V _{gr}	V _R	V _{J₂}	V _B	V _{J₁}	Observed	Gradient
28:0000			12	20	19		19	16	19	140	180
28:0600				19	19		19	14	19	140	050
28:1200				24	24		21	16	21	130	200
28:1800				12	12		13	6	13	160	190
29:0000				19	12		17	11	17	160	170
29:0600				6		11		3		200	170
29:1200				6	6	10	15	4	15	180	190
30:0600				40	40		21	25	21	140	190
30:1200				40	40		21	24	21	170	200
30:1800				32	25	12	17	16	17	180	240
October 1965											
01:0000	24			38	44	19	23	26	23	240	290
01:0600	25			48	31	10	23	30	23	280	320
01:1200	23			37	52	15	29	32	29	320	340
02:0600	17			40	40	16	21	26	21	220	260
02:1200	25			60	60	23	27	38	27	200	250
02:1800	23			48	39	13	22	22	22	220	280
03:0000	30			50	42	16	23	27	23	310	340
03:0600	30			45	39	26	21	26	21	330	360
03:1200				28	34		24	24	24	340	360
05:1200				16	20		19	14	19	150	190
05:1800	13	10		19	17	13	15	12	15	180	200
06:0000	18	18		28	26		21	19	21	160	220
06:0600	20			52	35	15	20	28	20	210	230
06:1200	23	19		33	33	15	19	22	19	190	220
06:1800	13			17	15		14	8	14	170	230

Cont 'd

Wind Speed (kts)

Date:Time (C.S.T.)	<u>Observed</u>			<u>Calculated</u>						<u>Wind Direction</u> (degrees)	
	16m	10m	7.5m	V _g	V _{gr}	V _R	V _{J2}	V _B	V _{J1}	Observed	Gradient
07:0000	12			21	22	17	17	13	17	190	210
07:0600	19			48	36		20	27	20	160	220
07:1200	24			35	26	17	17	18	17	180	240
07:1800	18			23	21	15	16	14	16	230	230
08:0000	22			50	43	19	24	26	24	280	300
08:0600	27			65	44	21	22	38	22	280	310
08:1200	27			45	31	19	19	26	19	290	310
08:1800	28			62	41	18	22	35	22	280	300
09:0000	21			50	36	13	20	29	20	310	320
09:0600	25			48	31	21	23	29	23	320	340
11:0600	9			15	21	13	16	10	16	310	340
11:1200	17			23	23	18	20	16	20	290	330
11:1800	19			26	24	12	17	16	17	300	300
12:0000	25			45	26	19	17	26	17	290	310
12:0600	28			43	39	13	25	29	25	300	320
22:1800	11	8	12	28	43	12	22	22	22	300	310
23:0000	20	18	19			11					
23:0600	19	17	14								
23:1200	22	20	25	42	63		33	37	33	350	350
23:1800			20	30	28		22	20	22	350	350
24:0000			16	52	44		27	40	27	350	360
24:0600	16		13	52	52		29	40	29	010	060
24:1200	11	11	14	19	19	13	19	14	19	330	350
24:1800	6	5	7	19	19	12	19	15	19	260	260
25:0000	20	18	18	34	31	15	23	26	23	240	360
25:0600	27	24	24	30	30	9	22	22	22	200	260

cont 'd

Wind Speed (kts)

Observed Calculated Wind Direction
 (degrees)
 Observed Gradient

Date: Time (C.S.T.) 16m 10m 7.5m V_g V_{gr} V_R V_{J₂} V_B V_{J₁}

25:1200	19	19	27	22	15	20	17	20		
25:1800			23	18	10	19	14	19		
29:0600	18	17	28	28	15	22	20	22		
29:1200	21	21	55	89	16	41	48	41		
29:1800	23	21	80	80	10	38	56	38		
30:0000	22	22	60	60	16	27	40	27		
30:0600	17	16	30	30	15	19	19	19		
30:1200	12	11	50	20	14	24	20	24		
30:1800		8	27	16	16	18	16	18		270
31:0000	22	22	62	54	19	27	32	27		350
31:0600	27	28	80	80	18	33	47	33		330
31:1200	21	22	53	53	18	27	31	27		330
31:1800	18	18	32	37	13	20	24	20		330

November 1965

01:0000	18	18	19	15	16	14	10	14		330
01:0600	12	13	37	23	16	16	20	16		310
01:1200	16	18	25	24	18	17	14	17		310
01:1800	7	7	19	19	11	15	13	15		280
03:0600	17	19	37	37		21	22	21		230
03:1200	19	20	48	43	24	22	28	22		230
03:1800					16					
04:0000					17					
04:0600					16					
04:1200					16					
04:1800			10	8			6			

cont'd

Wind Speed (kts)

<u>Observed</u>	<u>Calculated</u>						<u>Wind Direction</u> (degrees)
	<u>V_g</u>	<u>V_{gr}</u>	<u>V_R</u>	<u>V_{J2}</u>	<u>V_B</u>	<u>V_{J1}</u>	
Date:Time(C.S.T.)	16m	10m	7.5m				Observed Gradient
05:0000	9	8			5	14	190
05:0600	18	13		14	10	21	230
05:1200	25	16	13	21	13	16	250
05:1800	33	21	8	16	15	16	270
06:0000	23	19		16	12	14	270
06:0600	13	15		14	9	14	270

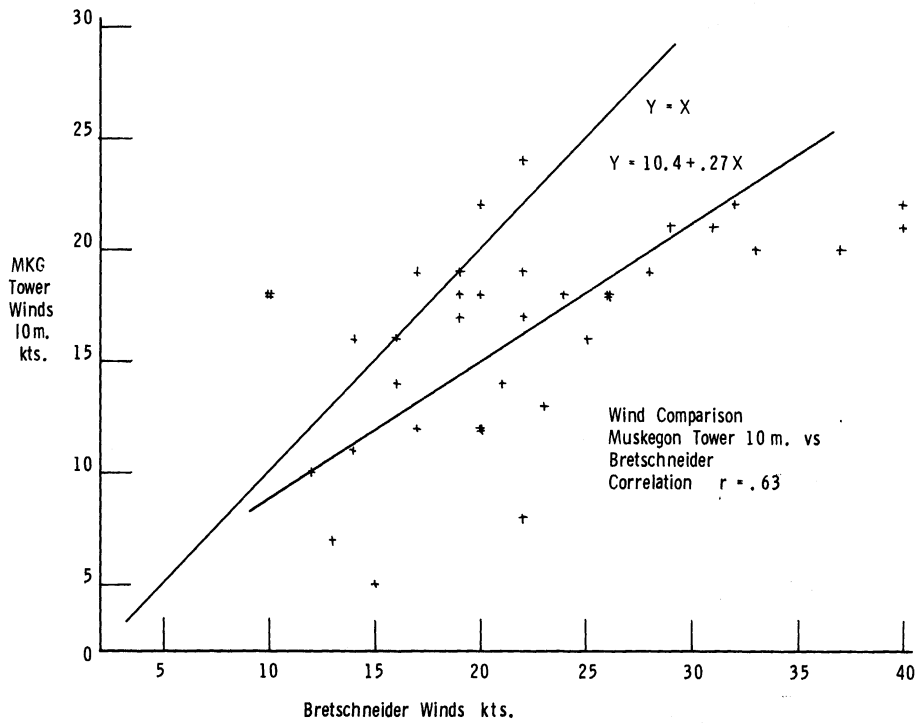


Figure A-1. Scatter diagram of Bretschneider winds vs. surface (10 meters) measured winds.

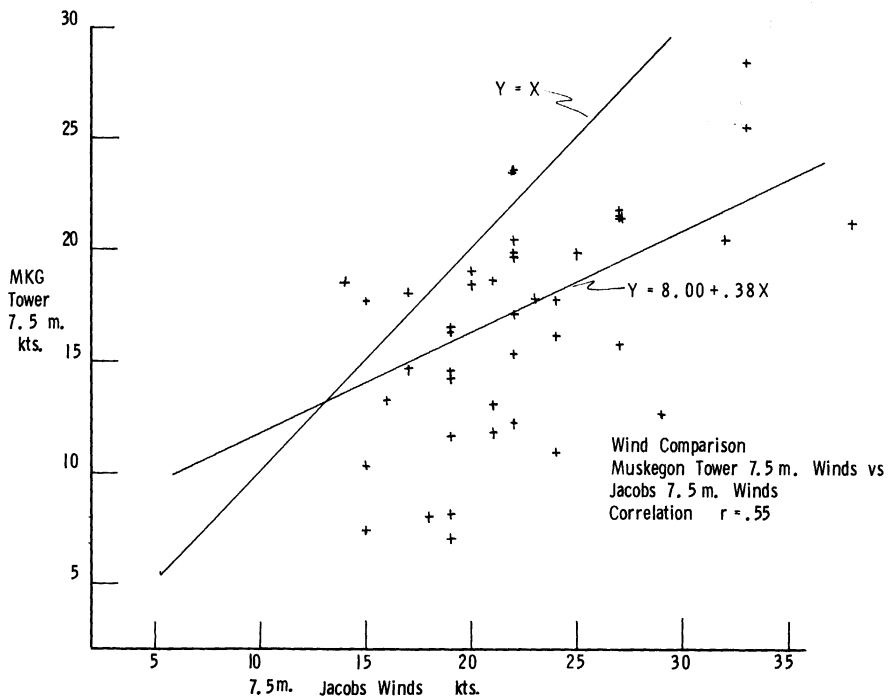
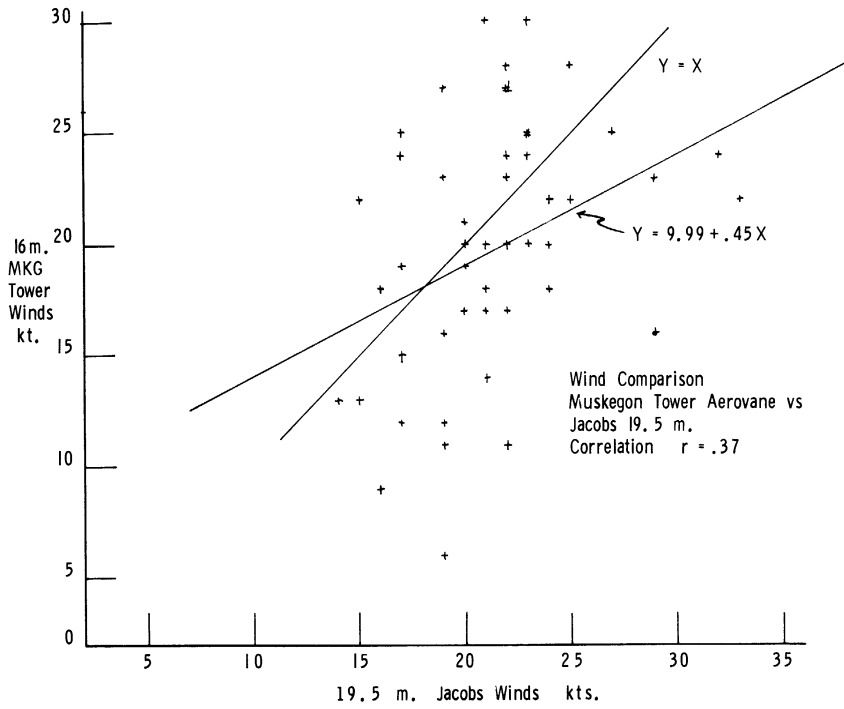


Figure A-2. Scatter diagram of the Jacobs 7.5 meter winds vs. surface (7.5 meters) measured winds.



A-3. Scatter diagram of the Jacobs 19.5 meter winds vs. surface (16 meters) measured winds.

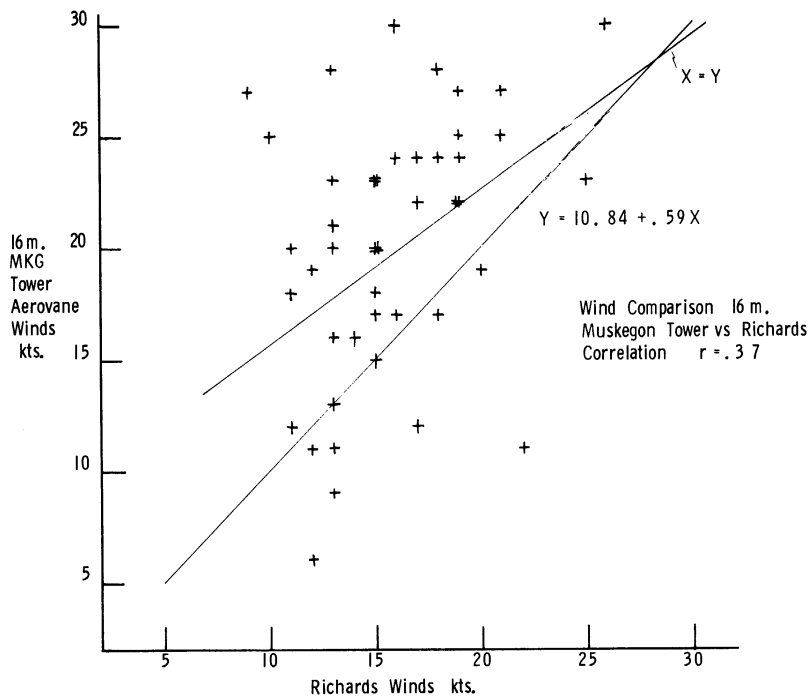


Figure A-4. Scatter diagram of the Richards winds vs. surface (16 meters) measured winds.

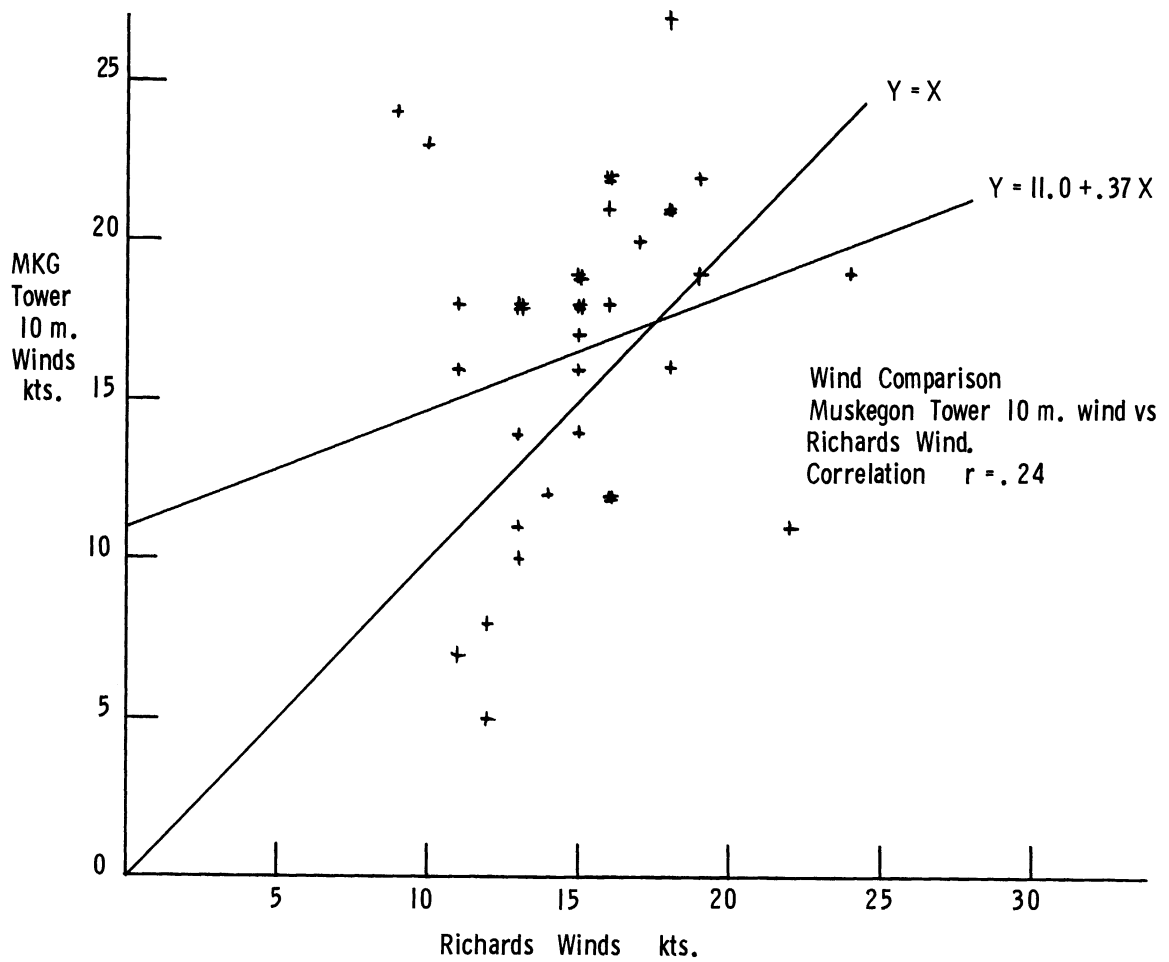


Figure A-5. Scatter diagram of the Richards winds vs. surface (10 meters) measured winds.

APPENDIX B

1965 WAVE DATA AND SCATTER
DIAGRAMS FOR MUSKEGON, MICHIGAN

TABLE B - 1

SIGNIFICANT WAVE HEIGHTS DURING 1965 HINDCAST PERIODS

Muskegon Research Tower

SMB B = SMB Wave Hindcasts with Bretschneider winds.

SMB R = SMB Wave Hindcasts with Richards winds.

SMB M = SMB Wave Hindcasts 10 meter measured winds.

PNJ J = PNJ Wave Hindcasts with Jacobs 7.5 measured winds.

PNJ R = PNJ Wave Hindcasts with Richards winds.

PNJ M = PNJ Wave Hindcasts with 7.5 meter measured winds.

PM J₂ = PM Wave Hindcasts with Jacobs 19.5 meter winds.

PM R = PM Wave Hindcasts with Richards winds.

PM M = PM Wave Hindcasts with 16 meter measured winds.

OBS = Significant wave heights as calculated from the standard deviation of the wave record.

OBS = Significant wave heights as calculated from the CERC spectra of the wave record.

CERC Abbreviations for sea state: FD=fully developed, FL = fetch limited, DL = duration limited and Sw = swell. All significant wave heights are in feet.

Date:Time C.S.T.	Sea State	SMB	SMB	SMB	SMB	PNJ	PNJ	PNJ	PNJ	PM	PM	PM	OBS	OBS
		B	R	M	J	R	M	J ₂	R	M	R	M	OBS	CERC
September 1965														
23:0000	DL	2.4	2.7	2.5	2.2	2.1	2.2						2.3	3.1
23:0600	FD	5.3	2.6	4.7	6.1	1.8	4.9	6.3	2.2	2.6			3.7	3.6
23:1200	FL	5.9	3.9	6.4	5.9	4.2	7.7						5.5	5.4
23:1800	DL	4.5	5.3	5.5	2.9	6.9	7.3						7.0	6.1
24:0000	FL	4.8	4.4	2.8	7.4	4.5	2.7			4.7	3.6		6.1	5.3
24:0600	FD	4.5	3.3	3.5	6.7	2.7	3.5	6.5	3.1	4.7			3.7	4.5
24:1200	FL	6.5	4.0	3.7	8.7	3.8	4.0			4.1	5.3		4.6	4.1
24:1800	FL	7.7	2.5	4.4	7.8	1.8	4.6			2.2	5.9		4.2	4.1
25:0000	FL	8.2	3.0	5.2	7.8	2.7	5.9			4.7	7.3		5.1	5.1
25:0600	FL	11.0	4.4	6.1	8.0	5.1	7.7			8.8			4.9	5.4
25:1200	FL	9.4	5.6	7.0	8.7	6.1	8.3			5.9	10.5		7.6	7.0
25:1800	FD	2.4		5.3	3.2	6.9	5.9	4.0	6.6	8.0			7.6	7.0
26:0000						5.1	1.9			2.2			4.6	4.6
26:0600	FL												3.1	2.0
28:0000	FL	2.5			2.2								2.4	2.1
28:0600	DL	3.6			7.1								2.9	2.3
28:1200	FD	4.7			8.4			7.7					2.9	2.4
28:1800	FD				2.5			3.3					2.7	2.4
29:0000	FL				8.2								1.7	1.1
29:0600	FL					1.5							1.0	.9
29:1200	FD		2.0		3.7	1.4		4.1	1.8				.9	
30:0600	DL	8.0			7.5								1.6	1.3
30:1200	FD	8.3			8.2			8.3					4.2	3.3
30:1800	FD	4.6			4.7	2.0		5.4					4.4	4.4

cont'd

Date:Time C.S.T.	Sea State	SMB		PNJ J	PNJ		PM J ₂	PM R	PM M	OBS	OBS CERC
		B	R		R	M					
October 1965											
01:0000	DL	5.1	3.4	2.3	5.1					5.0	5.5
01:0600	FL	8.7	2.2	9.7	1.4			1.8		7.3	7.3
01:1200	FL	1.9	3.2	8.9	3.6					5.8	1.2
02:0600	FL	8.3	2.5	7.5	2.2					2.4	2.5
02:1200	FL	13.2	5.6	8.2	7.6	2.0				5.8	5.8
02:1800	FD	7.7	3.5	6.8	2.7	4.7	9.0	3.1		6.9	5.1
03:0000	FL		4.5		4.5			4.7		5.6	4.6
03:0600	FL		7.3		7.3					7.1	6.2
03:1200	FL									3.6	2.9
05:1200	DL	3.4		7.2						.8	
05:1800	FD	2.8		3.3	2.1	2.1	4.0			2.0	2.3
06:0000	FD	4.5		9.1	.6	.6	8.2		5.9	3.3	4.0
06:0600	DL	8.0	2.2	6.9	2.2	5.0				5.8	5.3
06:1200	FD	7.4	3.7	6.4	3.8	8.9	6.9	4.1		7.6	6.0
06:1800	FD			2.2			3.7			4.4	3.0
07:0000	FD	3.5	2.8	2.7	2.2		5.1			2.2	2.0
07:0600	DL	7.1		5.7		2.1				3.7	3.5
07:1200	FD	5.4	2.8	4.8	2.2	.8	5.5		10.5	5.2	4.1
07:1800	FD	3.9	4.0	3.9	3.8	1.2	4.6	4.1	5.9	6.3	6.0
08:0000	DL	7.0	5.2	3.3	6.5					4.2	3.4
08:0600	DL	13.0	7.4	8.5	7.9	2.2				8.2	8.6
08:1200	FD	8.5	5.5	6.1	6.9	7.5	6.4	6.6		8.3	8.1
08:1800	FD	12.0	5.1	8.4	6.1	9.0	8.5	5.9	14.3	7.2	7.0
09:0000	FD	10.0	3.3	7.0	2.7	9.7	7.4	3.1	8.0	6.5	4.5
09:0600	FL		5.3	10.7	5.5	4.8			11.4	5.8	2.7
11:0600	FL				2.1					2.2	1.7

cont'd

Date:Time C.S.T.	Sea State	SMB		SMB		SMB		PNJ J	PNJ		PM J ₂	PM R	PM M	OBS	OBS CERC
		B	R	R	M	R	M								
11:1200	FD	4.7	4.0	2.7	8.1	4.9	7.4				2.4			2.2	
11:1800	FD	4.5	2.9	4.5	4.5	2.2	5.2				4.5	2.6		3.8	
12:0000	FD	8.6	4.5	7.0	4.9	5.1	5.5				5.2			5.5	
12:0600	DL	10.0	3.2	7.8	7.5	2.7					9.1	3.1		6.7	
22:1800	DL	3.9			2.2	2.0					1.8				
23:0000			2.4	3.2		1.8					3.6	2.2		3.4	
23:0600											4.1			2.4	
23:1200	FL	2.3									3.4			2.5	
23:1800	FL										4.8			3.2	
24:0000	FL	2.6									4.0			2.7	
24:0600	FL	2.6									2.3				
24:1200	FL	2.1									2.5			1.7	
24:1800	DL		2.7		1.6	2.2					1.9	2.6		1.0	
25:0000	FL	3.8	3.7	3.3		3.8					3.8	4.1		5.0	
25:0600	DL	4.6		4.6	2.2	1.1					7.3	1.5		7.5	
25:1200	DL,FL	4.6	3.2	5.9	7.5	3.1					3.3				
25:1800	FD	3.6	2.4		6.7	1.4	6.5				.5	1.8			
29:0600	FL	4.8	2.3	2.9	8.5	2.1					5.9			3.7	
29:1200	FL	14.8	3.9	5.5	12.3	4.5					7.9	4.7		6.9	
29:1800	FL	21.5	2.4	7.7	10.3	1.4					8.4	1.8		8.2	
30:0000	FL	14.2	3.6	7.6	8.0	4.5					8.4			6.7	
30:0600	FD	5.4	4.3	5.0	5.7	2.7					7.6	4.1		6.0	
30:1200	FL	6.0	3.9	3.1	7.8	3.2					5.5	3.6		4.3	
30:1800	FD	4.4			4.2	4.5	6.0				3.1	4.7		2.5	
31:0000	DL	9.0	4.5	4.0	6.3	2.1					4.3				
31:0600	FL	3.1	5.5	6.7		4.9					7.2	5.9		5.3	
31:1200	DL	6.3	3.5	4.2	2.3	2.2					7.6			5.6	
31:1800	FD	8.4	3.5	4.5	7.3	5.1	7.6				4.5	3.1		4.2	

cont'd

Date:Time Sea State
 C.S.T.

November 1965

Date:Time	Sea State	SMB B	SMB R	SMB M	PNJ J	PNJ R	PNJ M	PM J ₂	PM R	PM M	OBS	OBS CERC
01:0000	FD		4.4	5.4	3.0	2.0	4.2	3.7	4.7		3.3	2.7
01:0600	FD	4.2	4.4	2.8	4.2	1.8	2.8	4.9	4.7		3.0	2.2
01:1200	FD	3.8	5.2	3.6	4.4		5.0	5.1	5.9		3.6	2.7
01:1800	FD	3.2	2.5		3.6		6.1	4.3	2.2		2.5	1.8
03:0600	FD	7.0		2.7	7.4		.7	7.7			4.5	4.2
03:1200	FL	9.2	4.5	5.0	7.7		7.5				6.3	7.1
03:1800			4.4			2.1			4.7		5.5	4.7
04:0000			5.0			2.2			5.3		5.0	5.2
04:0600			4.7			3.8			4.7		3.5	2.7
04:1200			4.5			1.1			4.7		.9	
04:1800	FL					3.1					.8	2.2
05:0000						1.4					1.0	
05:0600	FD				2.7			3.4			3.7	
05:1200	DL	2.7			5.5	2.1					3.6	
05:1800	FD	3.8			3.1	5.3		4.8	1.2		2.9	
06:0000	FD	2.7			3.6			4.4			2.9	2.7
06:0600	FD				3.0	2.1		3.8			2.8	2.6
06:1200						4.5					1.7	
06:1800						1.4					.7	

TABLE B-2

SIGNIFICANT PERIOD OR PERIOD OF MAXIMUM ENERGY FOR 1965 WAVE HINDCAST TIMES

Muskegon Research Tower

SMB B = SMB Period hindcasts with Bretschneider winds.

SMB R = SMB Period hindcasts with Richards winds.

SMB M = SMB Period hindcasts with measured 10 meter winds.

PNJ J1 = PNJ Period hindcasts with Jacobs 7.5 meter winds.

PNJ R = PNJ Period hindcasts with Richards winds.

PNJ M = PNJ Period hindcasts with measured 7.5 meter winds.

PM J2 = PM Period hindcasts with Jacobs 19.5 meter winds.

PM R = PM Period hindcasts with Richards winds.

PM M = PM Period hindcasts with measured 16 meter winds.

OBS = Period of Maximum Energy as determined from the CERC spectra of the wave
CERC record.

Abbreviations for sea state: FD= Fully developed, FL= Fetch limited, DL= Duration Limited, and Sw= Swell. All periods are in seconds.

Date:Time Sea State SMB B SMB R SMB M PNB J1 PNB R PNB M PM J2 PM R PM M OBS CERC

September 1965

23:0000	DL	3.8	4.0	3.8	4.8	4.3	4.5											4.1
23:0600	FD	5.8	4.9	5.6	7.1	4.4	6.2											4.9
23:1200	FL	6.4	5.2	6.8	9.3	7.6	7.4											5.8
23:1800	DL	5.3	6.1	6.2	6.9	9.9	8.9											6.6
24:0000	FL	5.9	5.7	4.8	8.4	6.5	4.9											5.8
24:0600	FD	5.8	5.2	5.2	7.6	5.3	5.5											5.0
24:1200	FL	6.7	5.5	5.3	9.7	6.1	5.7											5.0
24:1800	FL	7.2	4.7	5.7	8.7	4.4	6.0											5.0
25:0000	FL	7.3	4.8	6.1	8.7	5.3	6.7											5.4
25:0600	FL	8.2	5.4	6.5	8.5	7.8	7.4											5.5
25:1200	FL	7.2	6.5	7.1	8.1	7.3	7.7											6.7
25:1800	FD	4.7		6.2	5.7	7.7	6.7											6.5
26:0000						9.4	6.9											
26:0600	FL																	
28:0000	FL	3.8			4.7													4.6
28:0600	DL	5.4			10.9													5.1
28:1200	FD	5.9			8.3													5.0
28:1800	FD				5.1													4.7
29:0000	FL																	
29:0600	FL		3.0			4.7												
29:1200	FD		4.5			4.0												
30:0600	DL	7.3																3.3
30:1200	FD	7.6			9.9													5.4
30:1800	FD	5.8			6.1	5.2												4.9

Date:Time C.S.T.	Sea State	SMB B	SMB R	SMB M	PNJ J ₁	PNJ R	PNJ M	PM J ₂	PM R	PM M	OBS CERC
October 1965											
01:0000	DL	5.2	4.3	4.8	4.7	6.3					5.6
01:0600	FL	7.6	4.5	6.8	13.0	4.0			3.8		6.6
01:1200	FL	2.7	4.7	6.8	8.3	7.2					6.5
02:0600	FL	7.5	3.8	3.8	9.3	4.3					3.9
02:1200	FL	8.7	5.9	6.0	8.6	7.9					5.7
02:1800	FD	6.7	5.4	6.8	7.7	5.3	8.4		4.9		6.8
03:0000	FL	2.4	5.7	7.4		6.5			6.0		5.3
03:0600	FL	2.4	6.7	8.3		6.8					7.3
03:1200	FL	2.3									4.5
05:1200	DL	5.0			10.9			5.5			3.1
05:1800	FD	5.0	3.3	2.8	5.7	5.1		8.0			3.9
06:0000	FD	5.4			8.6						4.7
06:0600	DL	6.9	3.7	4.2	10.6	4.3		7.3			6.2
06:1200	FD	7.2	5.2	6.0	7.9	6.1		5.4	5.6		6.7
06:1800	FD				5.3			6.2			5.9
07:0000	FD	5.6	4.0	3.0	6.1	4.1					4.0
07:0600	DL	6.5			8.9			6.5			4.5
07:1200	FD	6.3	4.0	4.8	7.1	4.1		6.0			5.6
07:1800	FD	5.7	5.5	6.2	6.1	6.1			5.6		6.0
08:0000	DL	6.5	6.0	6.2	5.8	5.3					5.0
08:0600	DL	8.6	6.6	6.8	10.0	9.1		7.1			6.7
08:1200	FD	7.4	6.3	7.2	7.3	7.7		8.1	7.1		6.7
08:1800	FD	8.3	6.1	7.4	8.3	7.3		7.5	6.8		6.4
09:0000	FD	8.0	5.2	6.6	8.1	5.3			4.9		5.9
09:0600	FL		5.9	7.2		6.3					
11:0600	FL		3.3	2.4		5.1					
11:1200	FD	6.1	5.1	4.2	8.2	6.8		7.6			3.7

cont'd

Date:Time	Sea	SMB	SMB	SMB	SMB	PNJ	PNJ	PNJ	PNJ	PNJ	PM	PM	PM	OBS
C.S.T.	State	B	R	M	J ₁	R	M	J ₂	R	M	R	M	M	CERC
11:1800	FD	5.7	4.9	5.5	6.5	4.8		6.3	4.5					5.0
12:0000	FD	7.5	5.4	6.7	6.7	6.5		6.6						5.6
12:0600	DL	8.0	5.2	7.2	8.3	5.3			4.9					6.9
22:1800	DL		3.2	2.4		5.1	5.1							
23:0000			4.5	4.4		4.4	6.2		4.1					
23:0600														
23:1200	FL													
23:1800	FL													
24:0000	FL													
24:0600	FL													
24:1200	FL													
24:1800	DL	3.6	3.3	2.9	4.7	5.2	4.4		4.5	6.8				
25:0000	FL	2.4	5.2	4.4		4.8	2.6		5.6					4.8
25:0600	DL	4.7	4.6	5.0	4.7	3.6	6.8		3.4					6.7
25:1200	DL,FL	5.8	4.7	6.6	10.0	5.7	8.4	7.9						
25:1800	FD	5.3	4.8		7.6	4.0			3.8					
							4.3							
							3.0			9.0				5.2
							3.9			4.5				
29:0600	FL	5.6	3.7	4.2	9.2	4.3	4.0							4.4
29:1200	FL	8.7	5.2	6.0	8.9	6.5	8.8		6.0					6.7
29:1800	FL	10.5	4.8	7.3	8.6	4.0	8.0		3.8	10.5				6.7
30:0000	FL	9.0	4.8	7.3	8.6	8.0	8.2			7.9				7.1
30:0600	FD	6.2	5.8	6.2	7.1	6.1	6.1		5.6	9.4				6.9
30:1200	FL	6.5	5.7	5.2	10.3	5.7	4.5		5.3					6.5
30:1800	FD	5.7			6.3	6.5	3.0	6.8	6.0					5.7
31:0000	DL	7.1	6.2	4.8	7.6	9.4	4.5							
31:0600	FL	3.1	6.4	6.8		7.3	6.7		6.8					6.2

cont'd

Date:Time C.S.T	Sea State	SMB		SMB		SMB		PNJ		PNJ		PNJ		PM		PM		OBS	
		B	R	M	J1	R	M	J2	R	M	J2	R	M	R	M	R	M	CERC	
31:1200	DL	5.8	4.7	5.0	4.6	5.3	5.1												7.8
31:1800	FD	7.6	5.5	5.5	7.9	5.3	8.8								7.7	4.9			5.7
November 1965																			
01:0000	FD		5.7	6.3	5.5	6.5	5.8								5.4	6.0			4.6
01:0600	FD	5.0	5.7	4.9	6.3	6.5	5.0								6.2	6.0			4.7
01:1200	FD	5.5	6.1	4.9	6.1	7.3	6.8								6.2	6.8			4.9
01:1800	FD	5.1	4.7		5.9	4.4	2.8								5.8	4.1			4.3
03:0600	FD	7.0		4.0	7.9		4.0								7.7				5.4
03:1200	FL	7.6	5.0	5.8	10.1	8.1	9.2												6.6
03:1800			5.7		6.5	6.5										6.0			
04:0000			6.2		6.9	6.9										6.4			
04:0600			6.0		6.5	6.5										6.0			
04:1200			5.8		6.5	6.5										6.0			
04:1800	FL																		
05:0000																			
05:0600	FD	3.4			5.3										5.2				
05:1200	DL	4.4	3.6		7.8	5.1													
05:1800	FD	5.3			5.6	3.2									6.1	3.0			5.0
06:0000	FD	4.8			5.9										5.8				4.1
06:1200																			
06:1800						6.3													

TABLE B-3

PERIOD BAND AND MAXIMUM WAVE HEIGHT
FOR 1965 WAVE HINDCAST TIMES

PNJ = Period band and maximum wave height in preceding 20 minutes as calculated from PNJ wave hindcasting method, using Jacobs' 7.5 meter wind.
PM = Period band as calculated from wave hindcasts based on PM spectra.
OBS = Maximum wave height as determined from wave spectra of wave gauge record.

Date:Time	Period Band (sec)		Maximum Wave Height (ft)	
	PNJ	PM	PNJ	OBS
	September 1965			
23:0000	1.0- 4.8		3.8	3.7
23:0600	2.4- 9.8	2.8-7.0	10.6	4.5
23:1200	2.9- 9.3		10.2	7.5
23:1800	2.5- 6.9		5.0	7.4
24:0000	3.1- 8.4		12.8	7.3
24:0600	2.8-10.4	2.8-7.0	11.6	5.7
24:1200	3.3- 9.7		15.1	4.8
24:1800	3.1- 8.7		13.5	5.2
25:0000	3.1- 8.7		13.5	6.2
25:0600	3.1- 8.5		13.9	7.4
25:1200	3.1- 8.1		15.1	9.9
25:1800	1.5- 7.8	2.2-5.5	5.5	9.3
28:0000	1.0- 4.7		3.8	2.8
28:0600	3.0-10.9		12.3	3.8
28:1200	3.1-11.4	3.1-7.7	14.6	2.9
28:1800	1.1- 7.2	1.8-4.6	4.3	3.1
29:0000			14.2	1.4
				cont'd

Date:Time	Period Band (sec)		Maximum Wave Height (ft)	
	PNJ	PM	PNJ	OBS
29:1200	1.8- 8.3	2.2-5.6	6.4	-
30:0600	3.0- 9.9		13.0	1.7
30:1200	1.8- 8.3	3.2-8.1	14.2	3.9
30:1800	2.1- 9.0	2.5-6.5	8.1	4.6
October 1965				
01:0000	1.3- 4.7		4.0	6.6
01:0600	3.5-13.0		16.8	9.6
01:1200	3.2- 8.3		15.4	5.6
02:0600	3.0- 9.3		13.0	3.8
02:1200	3.1- 8.6	3.3-8.4	14.2	8.7
02:1800	2.8-10.5		11.8	6.7
05:1200	3.0-10.9	2.2-5.6	12.5	-
05:1800	1.5- 7.8	3.1-8.0	5.7	2.9
06:0000	3.2- 7.5		15.8	7.5
06:0600	3.0-10.6	2.9-7.3	12.0	7.5
06:1200	2.4-10.2	2.1-5.4	11.1	9.0
06:1800	1.0- 7.0	2.5-6.2	3.8	3.7
07:0000	1.5- 8.3		4.7	3.0
07:0600	2.8- 8.9	2.6-6.5	9.9	4.6
07:1200	2.1- 9.1	2.4-6.0	8.3	5.0
07:1800	1.8- 8.3		6.7	7.0
08:0000	1.4- 5.8		5.7	4.7
08:0600	3.1-10.0	2.8-7.1	14.7	11.1
08:1200	2.5-10.0	3.2-8.1	10.6	10.8
				cont'd

Date:Time	Period Band (sec)		Maximum Wave Height (ft)	
	PNJ	PM	PNJ	OBS
08:1800	3.1-11.4	3.0-7.5	14.6	9.6
09:0000	2.8-10.5		12.1	6.0
09:0600	3.6		18.5	7.2
11:1200	3.0-11.2	3.0-7.5	14.0	3.1
11:1800	2.0- 8.8	2.5-6.3	7.8	4.5
12:0000	2.2- 9.1	2.6-6.6	8.5	6.9
12:0600	3.0- 8.3		13.0	10.3
12:1800	0.9- 4.7		3.8	-
25:0600	0.9- 9.1		3.8	10.1
25:1200	3.1-10.0		13.0	-
25:1800	2.8-10.4	2.8-7.1	11.6	
29:0600	3.2- 9.2		14.7	4.1
29:1200	3.7- 8.9		21.2	7.0
29:1800	3.5- 8.6		17.8	9.9
30:0000	3.1- 8.6		13.8	8.7
30:0600	2.4- 9.7		9.9	9.0
30:1200	3.1-10.3		13.5	5.4
30:1800	1.9- 8.5	2.7-6.8	7.3	9.5
31:0000	2.9- 7.6		10.9	
31:1200	0.9- 4.6		4.0	6.4
31:1800	2.9-10.8	3.0-7.7	12.6	4.5

cont'd

Date:Time	Period Band (sec)		Maximum Wave Height (ft)
	PNJ	PM	
November 1965			
01:0000	1.4- 7.6	2.1-5.3	5.2 3.1
01:0600	1.9- 8.5	2.4-6.2	7.3 2.7
01:1200	1.8- 8.1	2.5-6.2	7.6 6.2
01:1800	1.7- 8.1	2.3-5.8	6.2 2.3
03:0600	2.9-10.8	3.0-7.7	12.8 5.0
03:1200	3.1-10.1		13.3 8.8
05:0600	1.2- 7.4	2.0-5.1	4.7
05:1200	2.7- 7.8		9.5
05:1800	1.5- 7.7	2.4-6.1	5.4 2.8
06:0000	1.7- 8.1	2.3-5.8	6.2 3.1
06:0600	1.4- 7.6	2.1-5.4	5.2 3.1

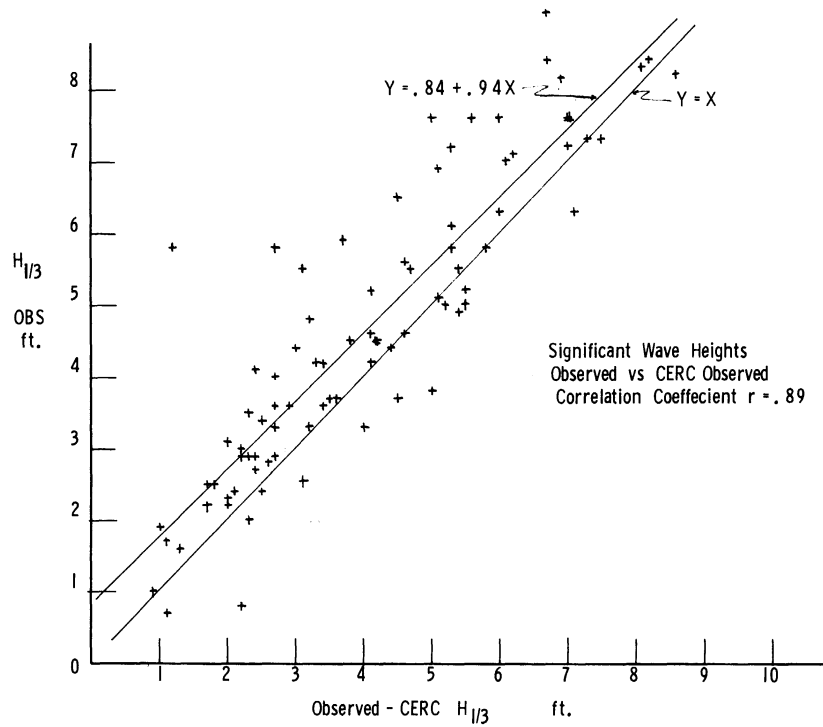


Figure B-1. Scatter diagram of CERC observed significant wave heights vs. those calculated from the standard deviation of the staff gage data.

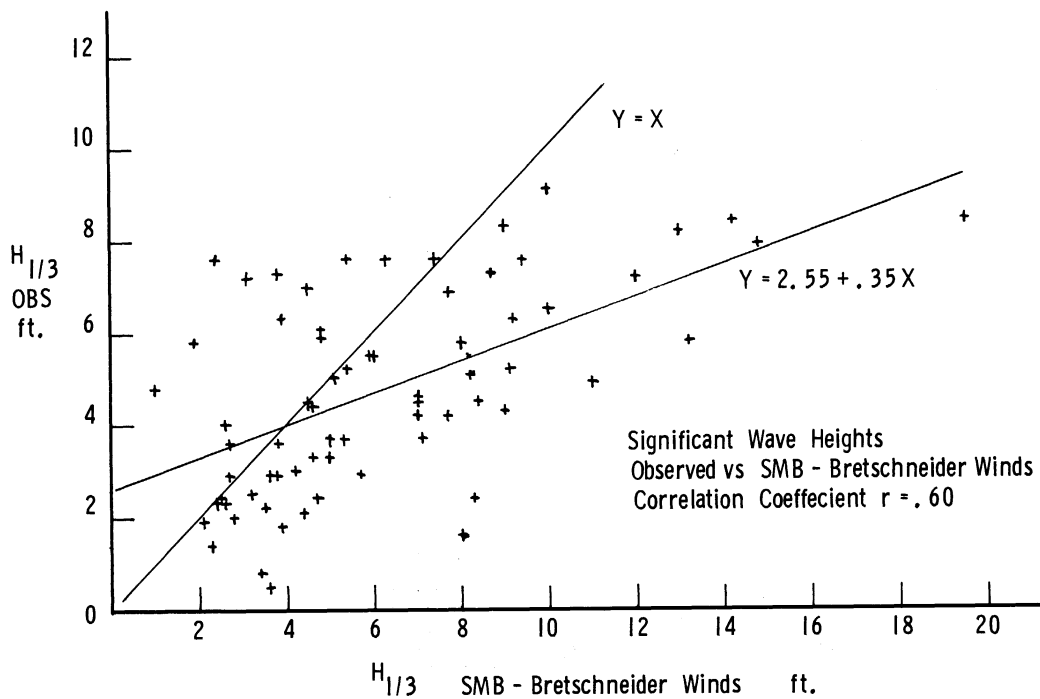


Figure B-2. Scatter diagram of hindcast significant wave heights calculated by the SMB (Bretschneider winds) method vs. the observed significant wave heights.

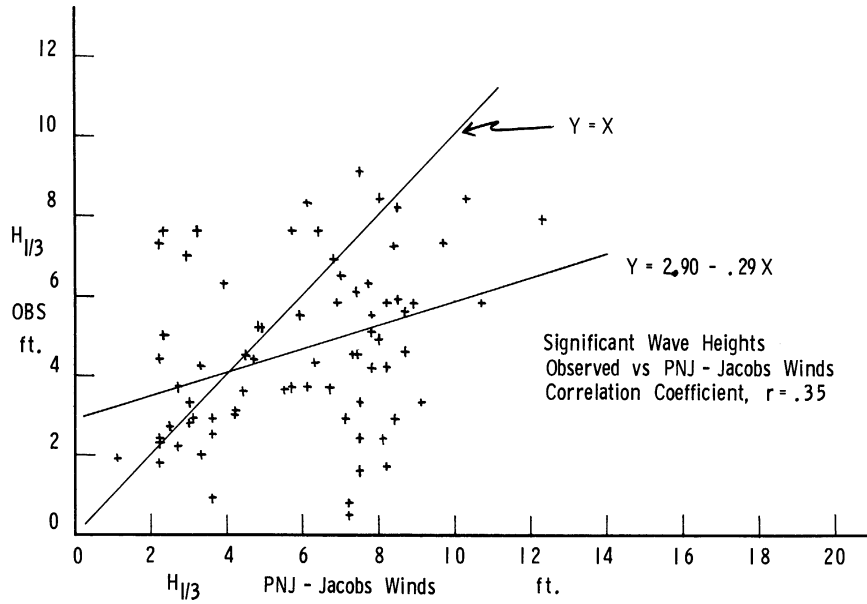


Figure B-3. Scatter diagram of hindcast significant wave heights calculated by the PM (Jacobs 7.5 meter winds) method vs. the observed significant wave heights.

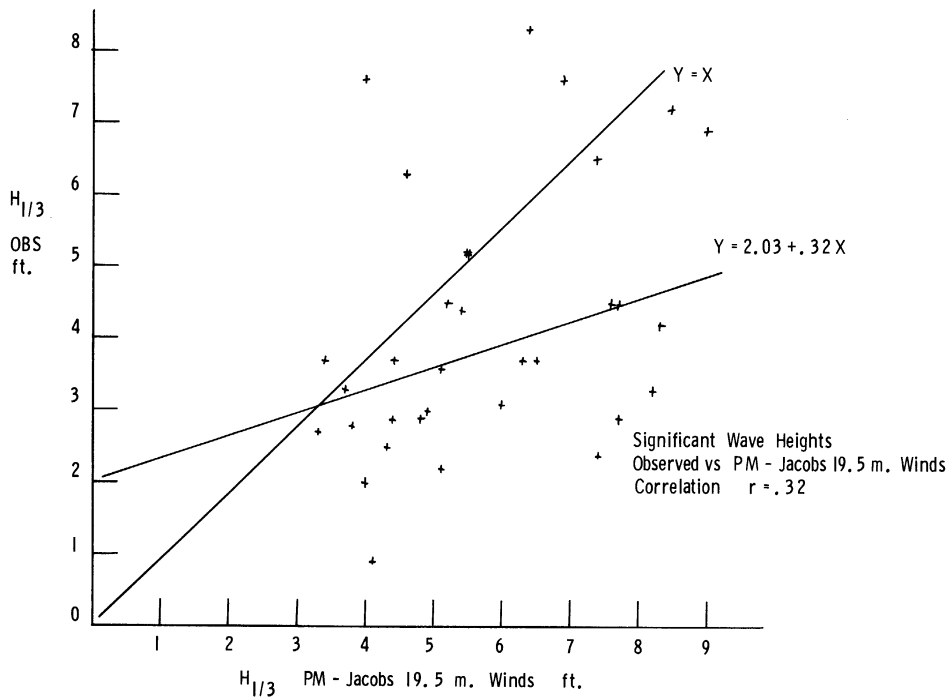


Figure B-4. Scatter diagram of hindcast significant wave heights calculated by the PM (Jacobs 19.5 meter winds) method vs. the observed significant wave heights.

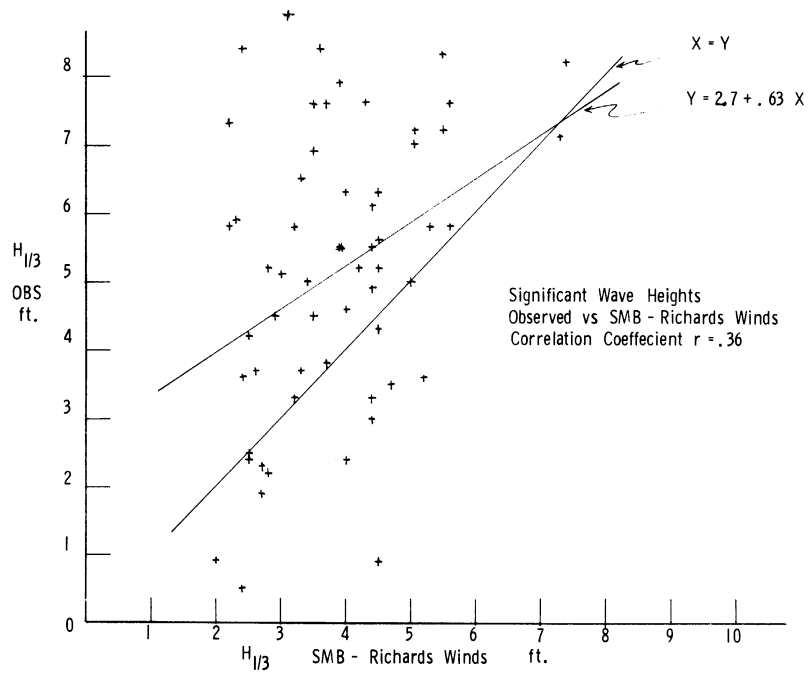


Figure B-5. Scatter diagram of hindcast significant wave heights calculated by the SMB (Richards winds) method vs. the observed significant wave heights.

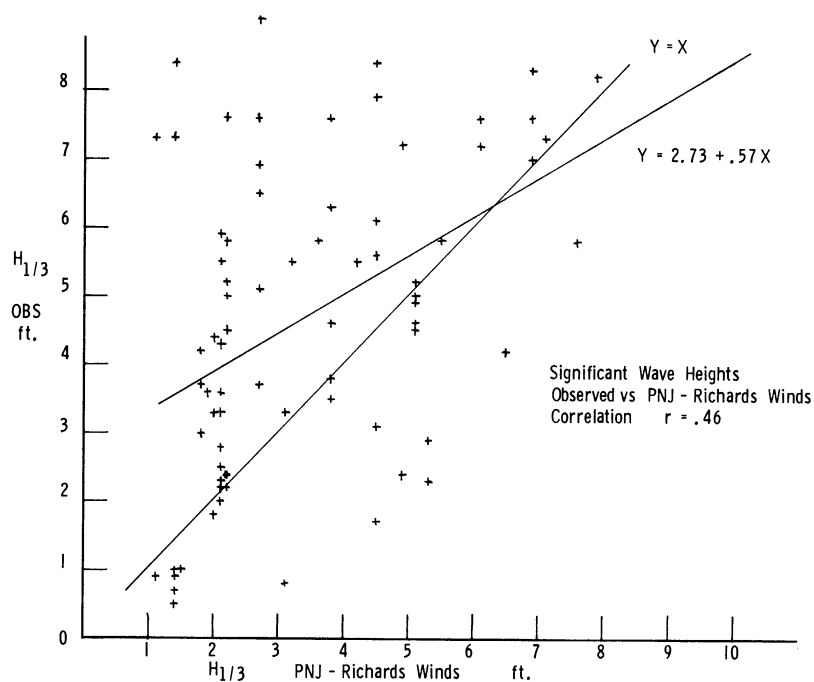


Figure B-6. Scatter diagram of hindcast significant wave heights calculated by the PNJ (Richards winds) method vs. the observed significant wave heights.

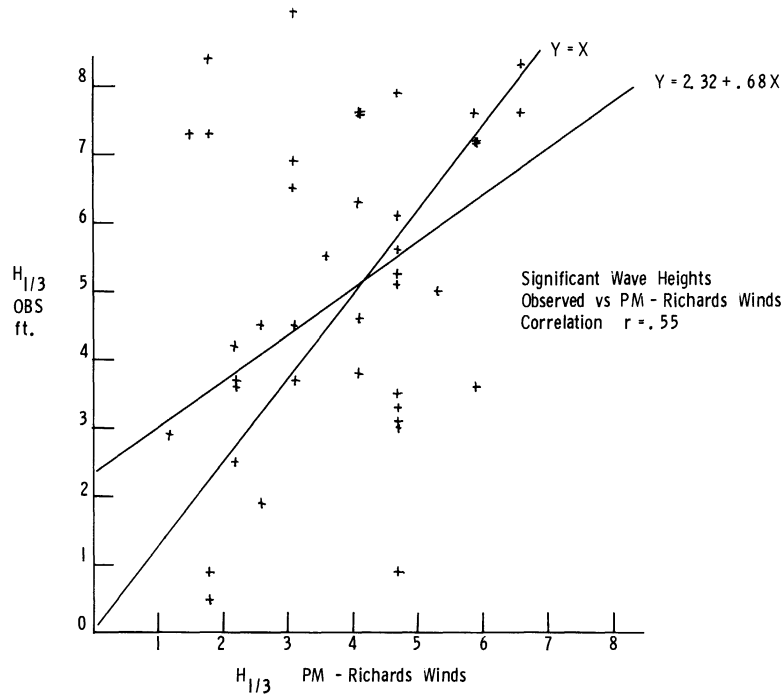


Figure B-7. Scatter diagram of hindcast significant wave heights calculated by the PM (Richards winds) method vs. the observed significant wave heights.

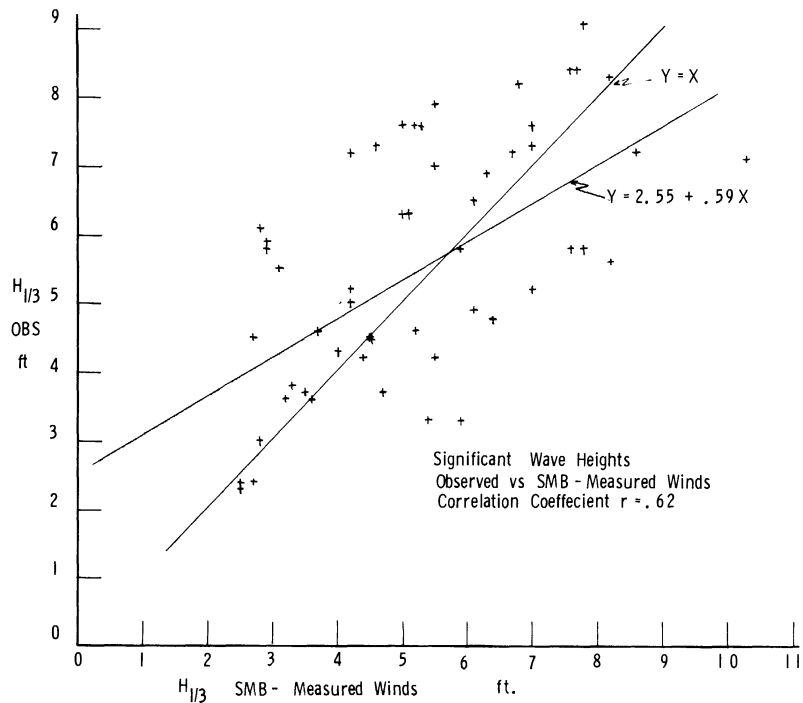


Figure B-8. Scatter diagram of hindcast significant wave heights calculated by the SMB (measured winds) method vs. the observed significant wave heights.

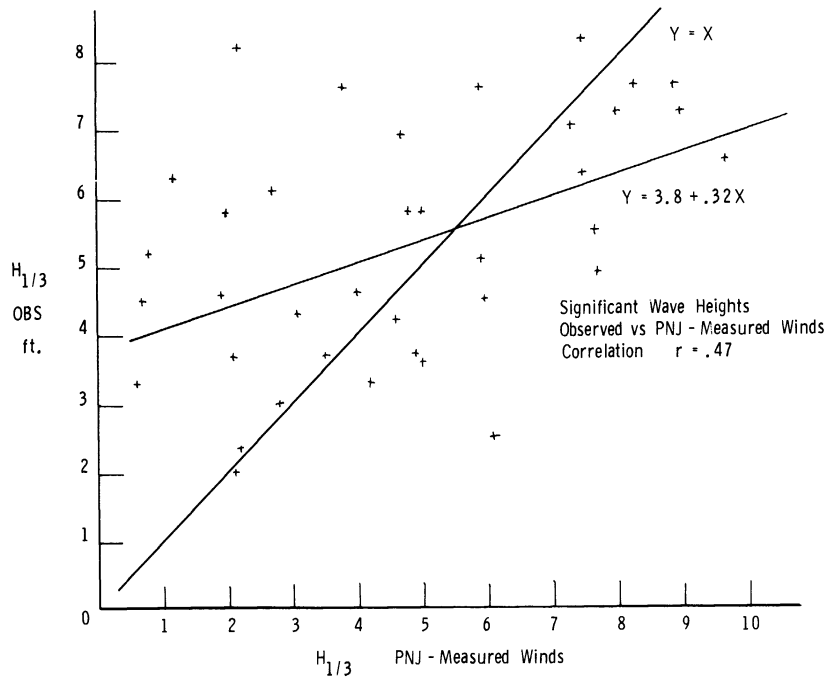


Figure B-9. Scatter diagram of hindcast significant wave heights calculated by the PNJ (measured winds) method vs. the observed significant wave heights.

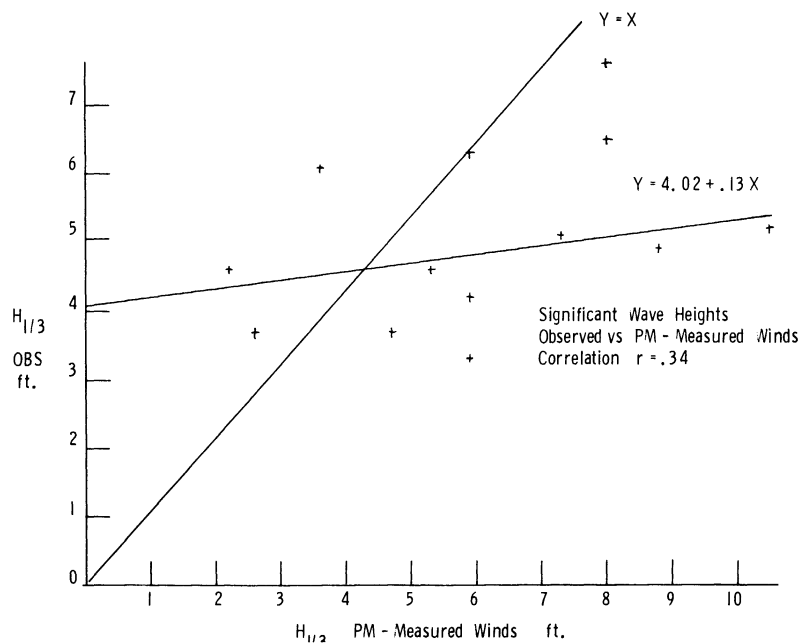


Figure B-10. Scatter diagram of hindcast significant wave heights calculated by the PM (measured winds) method vs. the observed significant wave heights.

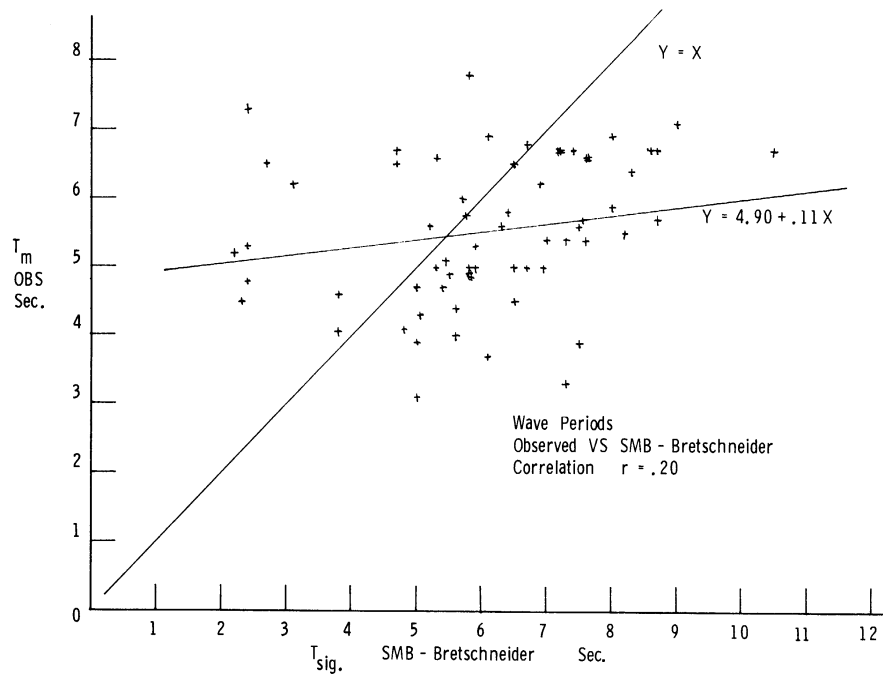


Figure B-11. Scatter diagram of hindcast significant period calculated by the SMB (Bretschneider winds) method vs. the observed period of maximum energy.

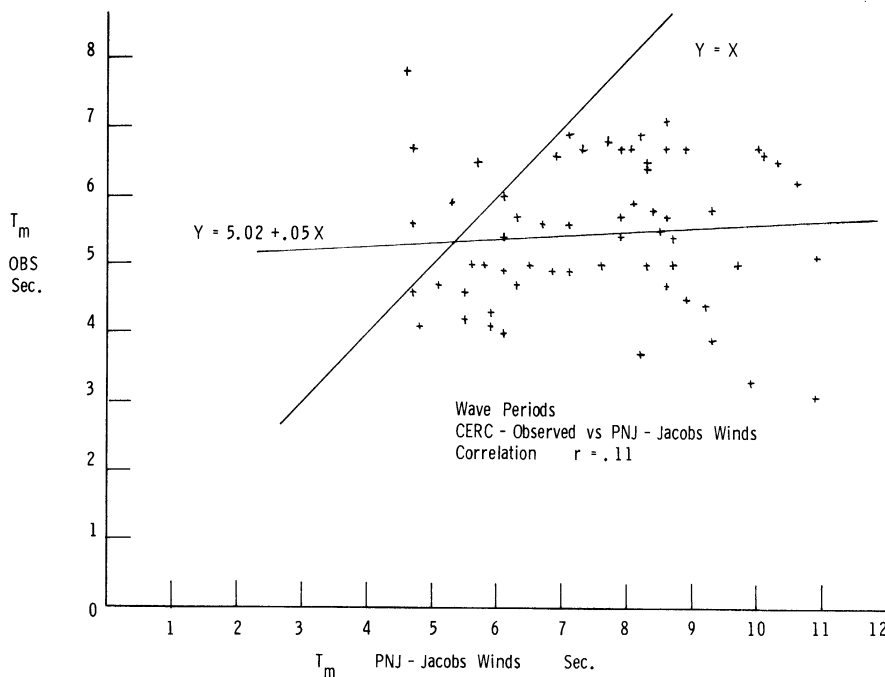


Figure B-12. Scatter diagram of hindcast period of maximum energy calculated by the PNJ (Jacobs' 7.5 meter winds) method vs. the observed period of maximum energy.

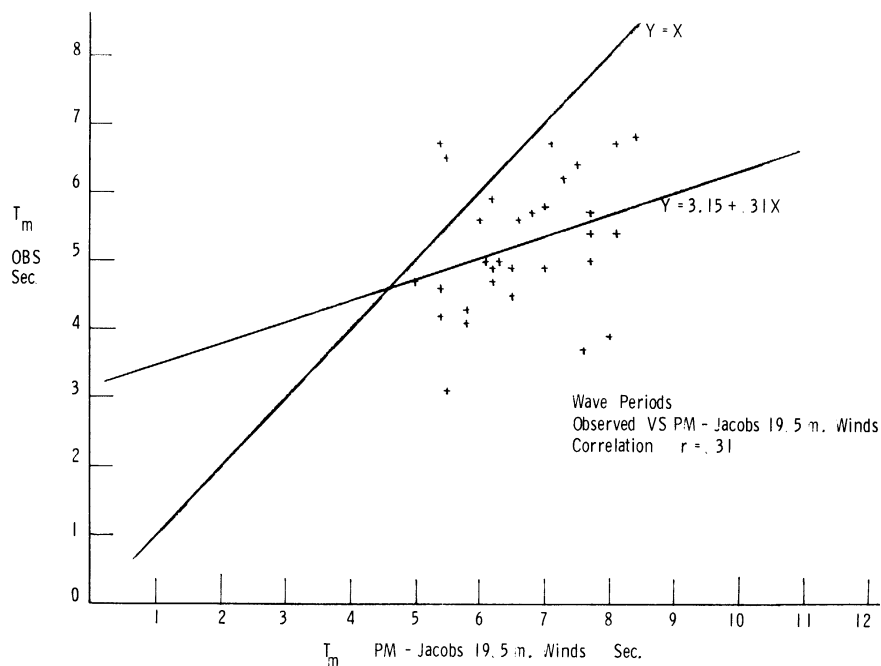


Figure B-13. Scatter diagram of hindcast period of maximum energy calculated by the PM (Jacobs' 19.5 meter winds) method vs. the observed period of maximum energy.

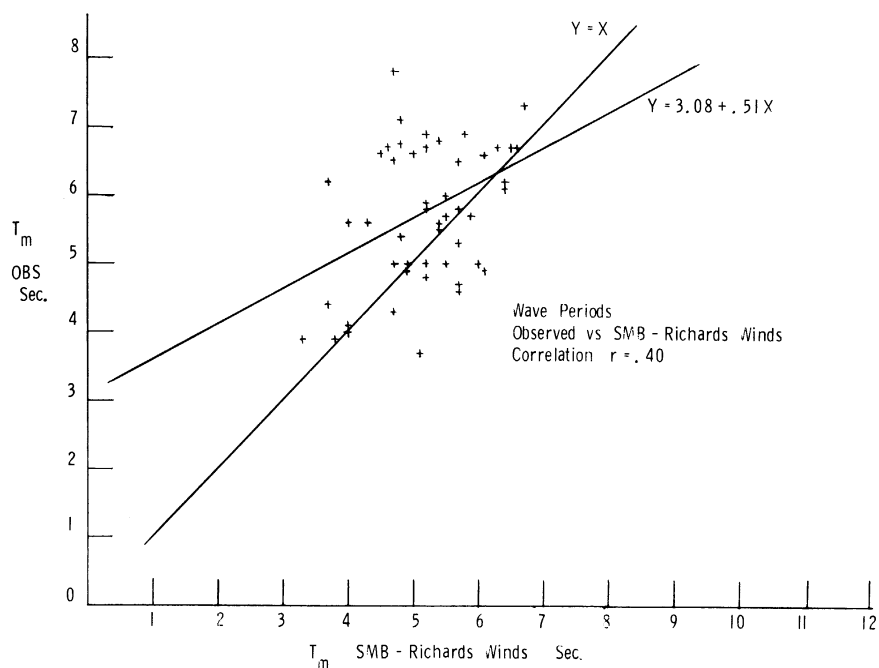


Figure B-14. Scatter diagram of hindcast significant period calculated by the SMB (Richards' winds) method vs. the observed periods of maximum energy.

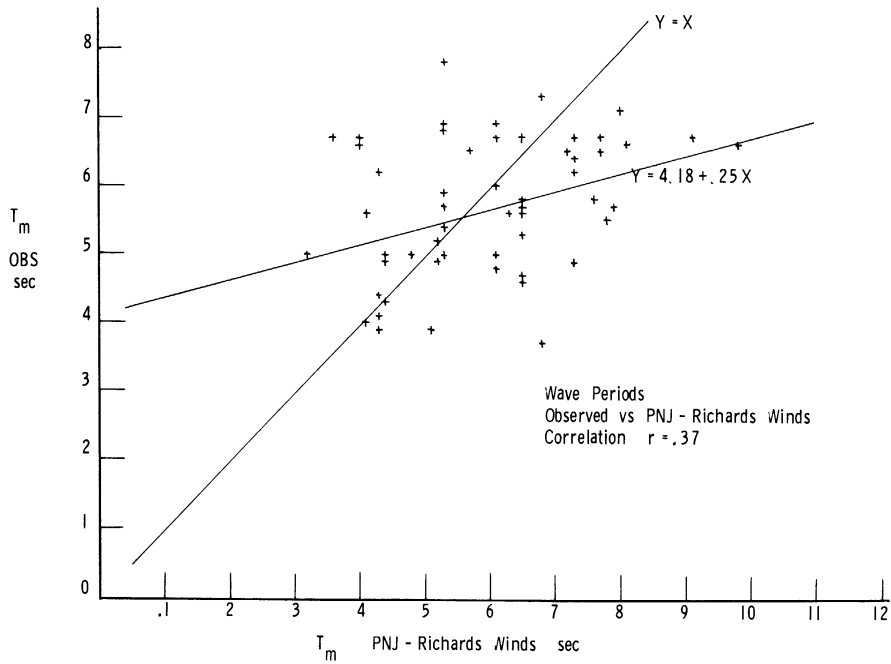


Figure B-15. Scatter diagram of hindcast of period of maximum energy calculated by the PNJ (Richards winds) method vs. the observed period of maximum energy.

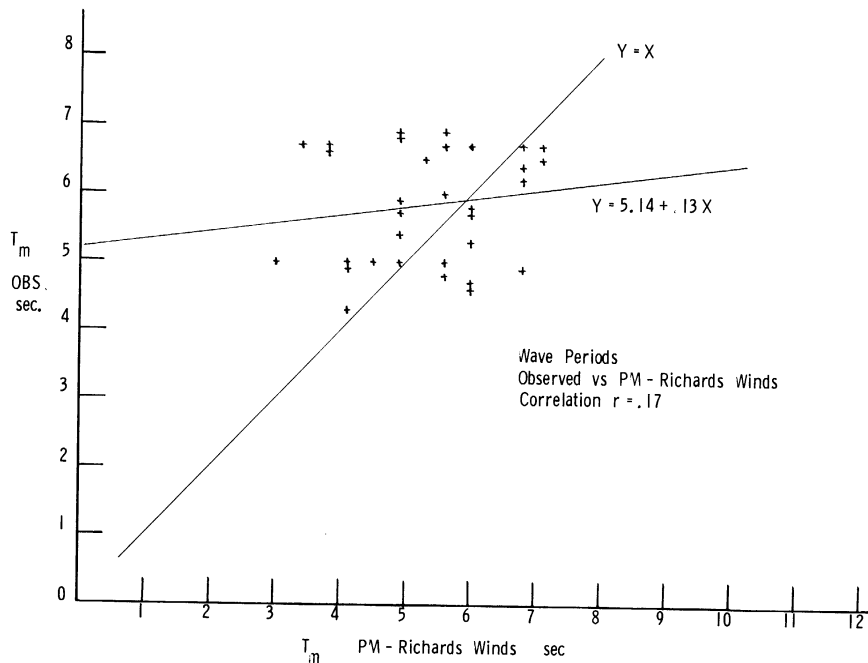


Figure B-16. Scatter diagram of hindcast of period of maximum energy calculated by the PM (Richards winds) method vs. the observed period of maximum energy.

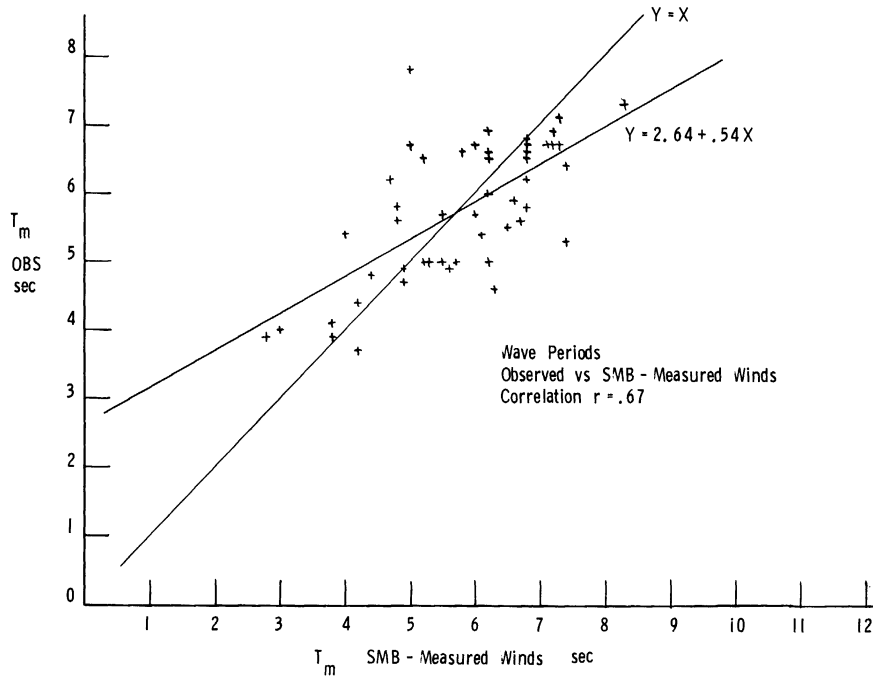


Figure B-17. Scatter diagram of hindcast significant wave period calculated by the SMB (measured winds) method vs. the observed period of maximum energy.

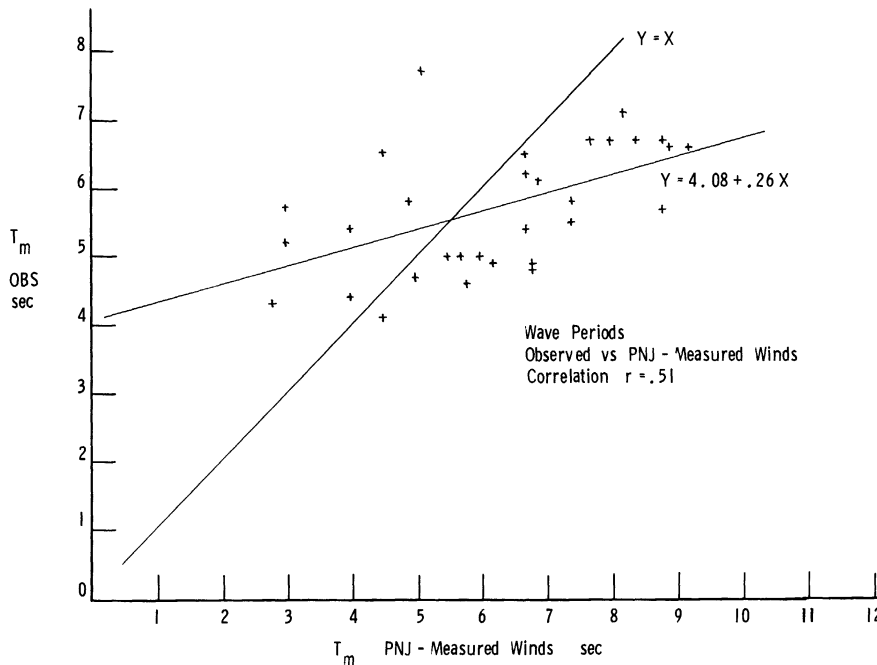


Figure B-18. Scatter diagram of hindcast wave period of maximum energy calculated by the PNJ (measured winds) method vs. the observed period of maximum energy.

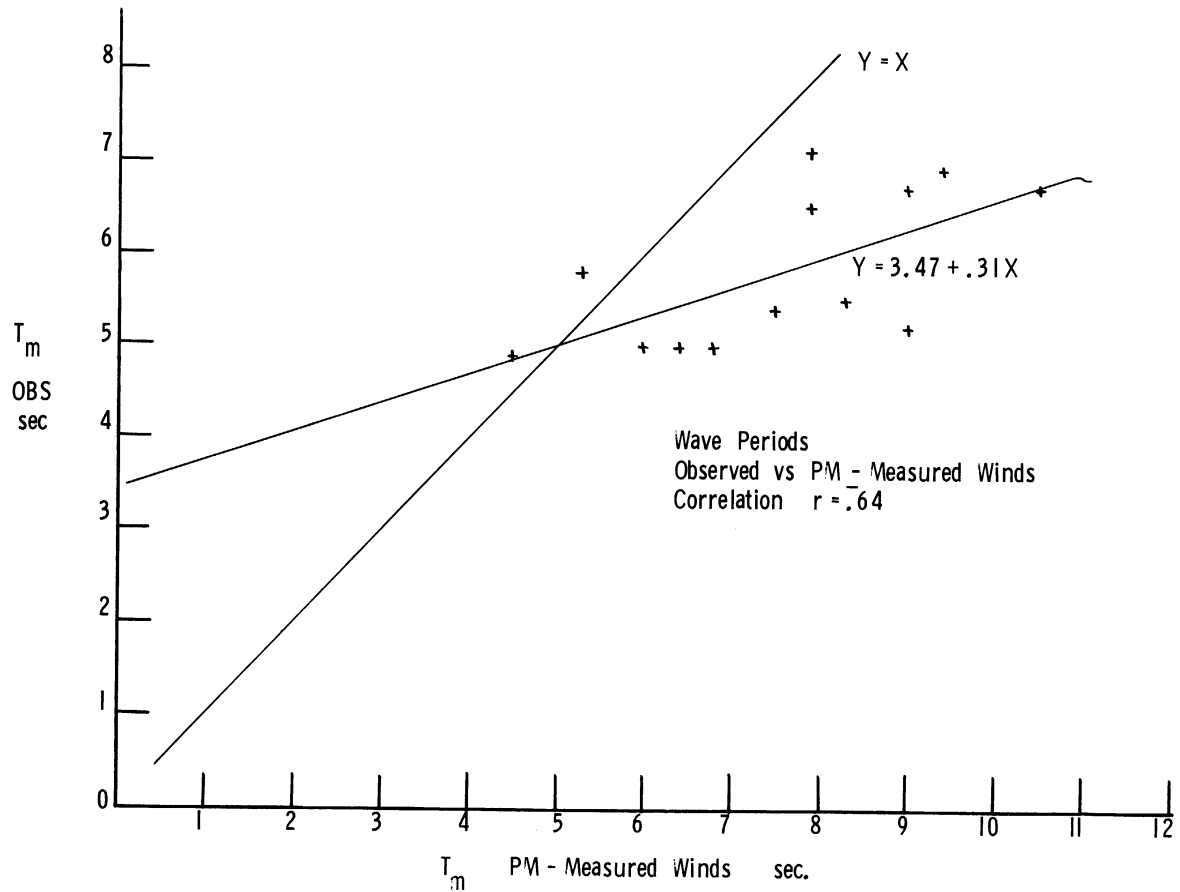


Figure B-19. Scatter diagram of hindcast wave period of maximum energy calculated by the PM (measured winds) method vs. the observed period of maximum energy.

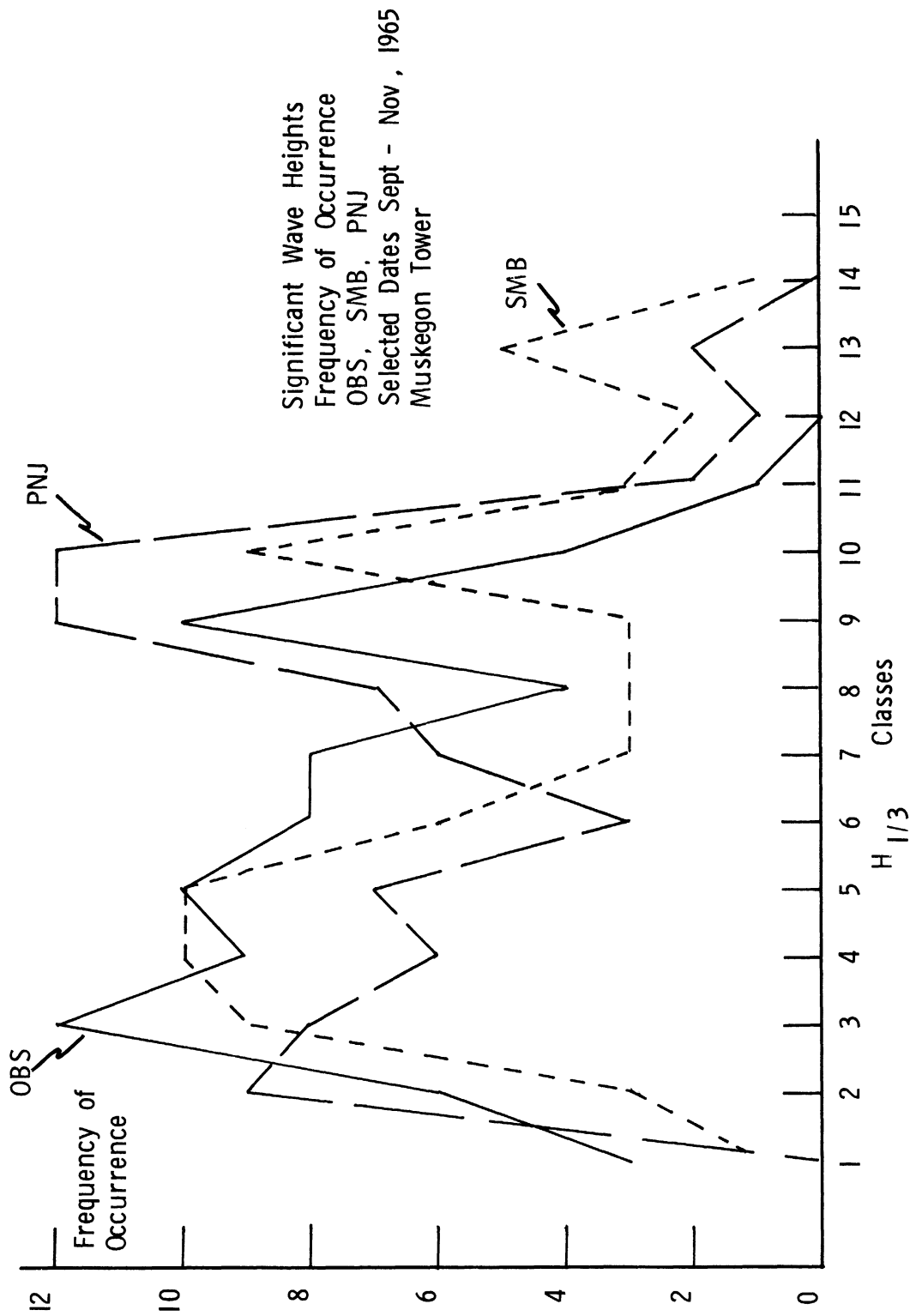


Figure B-20. Frequency distribution of significant wave heights as calculated by the SMB-Bretschneider wind method and the PNJ-Jacobs 7.5 meter wind method and as observed by the staff wave gage.

APPENDIX C
1965 WAVE DATA FOR POINT BETSIE
AND PORT HURON, MICHIGAN

TABLE C - 1

SIGNIFICANT WAVE HEIGHTS AND PERIODS
FOR 1965 WAVE HINDCAST TIMES
Point Betsie, Michigan

SMB Wave Hindcasts

Date:Time C.S.T.	Significant Wave Height (ft)	Significant Wave Period (sec)
28:0600	3.4	4.5
28:1200	5.3	6.2
October, 1965		
23:1200	6.2	5.8
23:1800	19.0	9.9
24:0000	6.2	6.7
24:0600	8.4	7.2
24:1200	3.1	5.0
24:1800	4.1	5.4
25:0000	7.0	6.5
25:1200	4.7	5.5
November, 1965		
01:0000	4.0	4.8
01:0600	6.4	6.4
01:1800	1.9	4.2
05:0600	5.3	5.5
05:1200	8.0	7.0
05:1800	5.0	5.7
06:0000	2.8	4.5

TABLE C - 2

SIGNIFICANT WAVE HEIGHTS AND PERIODS
 FOR 1965 WAVE HINDCAST TIMES
 Port Huron, Michigan

SMB Wave Hindcasts

Date:Time	Significant Wave Heights(ft)	Significant Wave Periods(sec)
October, 1965		
23:1200	4.2	4.8
28:1800	6.0	6.2
24:0000	7.5	7.0
24:1200	13.5	9.3

APPENDIX D

COMPARISON OF 1964 WAVE DATA
AT MUSKEGON, MICHIGAN

TABLE D-1

COMPARISON OF SMB, PNJ, PM AND OBS WAVE
DATA FOR 1964 HINDCAST PERIODS
Muskegon Research Tower

SMB = SMB Wave Hindcasts with Bretschneider Winds

PNJ, PM and OBS are taken from Jacobs (1965)

Date:Time C.S.T.	Sea	Significant Wave Height				Period of Maximum Energy			
		SMB	PNJ	PM	OBS	SMB	PNJ	PM	OBS
August, 1964									
01:0600	FD	5.2	3.8	4.7		5.3	6.1	6.0	
01:1200	FD	5.5	4.5	5.3		6.4	6.5	6.4	
01:1800	FD	4.9	3.2	4.1		6.2	5.7	5.6	
02:0600	FD	3.2	2.7	4.1		5.1	5.3	5.6	
02:1200	FD	4.5	3.2	4.7		5.5	5.7	6.0	
02:1800		5.6				6.3			
02:1926	Sw		3.2	4.7	1.6		5.7	6.0	4.2
07:0600		4.1				5.0			
07:0726	Sw		3.2	4.1	2.2		5.7	5.6	4.6
07:1200	FD	4.7	3.8	4.7		5.8	6.1	6.0	
07:1736	FD		3.8	4.7	1.7		6.1	6.0	4.6
07:1800		2.6				4.8			
10:1200		3.2				4.4			

Significant Wave Height Period of Maximum Energy

Date:Time	Sea	SMB	PNJ	PM	OBS	SMB	PNJ	PM	OBS
C.S.T.									
10:1330	Sw		3.2	4.1	1.9		5.7	5.6	3.8
10:1530	Sw		3.2	4.1	2.0		5.7	5.6	4.2
10:1800		5.1				5.9			
10:1950	Sw		3.0	4.0	1.7		5.7	5.6	5.0
11:0000		7.4				7.0			
September, 1964									
13:0000		0	0	0	0				
13:0600	FD	2.5	1.2	1.6	0	3.8	3.8	3.5	
13:1200	FD	3.7	2.2	3.1	1.8	5.3	4.8	4.9	
13:1800	FD		1.8	3.1	1.6		4.4	4.9	
14:0000	FD	2.7	3.2	4.1	2.7	4.3	5.3	5.6	
14:0600	FD	4.5	4.5	5.3	3.2	5.4	6.5	6.4	
20:1200	FL	3.4	2.8		0.6	4.4	5.5		
20:1800	FL	4.3	2.8		0.8	5.4	5.9		
21:0000	FL	2.6	3.0		2.0	4.8	5.0		4.8
21:0100									
21:0300					3.8				
21:0500									5.6
21:0600	FD	2.9	3.8	4.7	1.4	4.4	6.1	6.0	4.8
21:0900									
23:0000	FL	6.6	0.9		0.6	5.9	2.5		
23:0300					0.9				
23:0600	DL	7.7	2.8		2.8	6.3	4.0		5.7
23:0700									
23:0900									
23:1100					6.6				7.0

Date:Time C.S.T.	Significant Wave Height				Period Of Maximum Energy				
	Sea	SMB	PNJ	PM	OBS	SMB	PNJ	PM	OBS
23:1200	DL	4.8	5.7		6.3	5.2	7.0		7.8
23:1500							6.5		
23:1800	FL	9.0	9.0		7.5	7.5	6.0		8.2
23:1900							6.4		8.3
23:2000							6.8		8.6
23:2100					8.7		7.3		8.7
23:2200							7.7		8.9
23:2300							8.1		8.9
24:0000	FL	4.7	9.0			5.8	8.5		8.9

APPENDIX E

SUCCESSIVE APPROXIMATION TECHNIQUE
FOR ANALYSIS OF PRESSURE AND WIND FIELDS

APPENDIX E

Successive Approximation Technique for Pressure and Geostrophic Wind Analysis

Introduction

The successive approximation technique, hereafter called SAT, is an objective analysis method of computing data at the points of a regularly arranged grid from measurements taken at irregularly spaced locations. Figure E-1 illustrates the grid and the location of weather stations used in the analysis. The gridpoint array is 18 x 17 (306 gridpoints) with a 75 km (\approx 40 n. mi.) spacing. For geostrophic wind calculations, the grid system reduces to 16 x 15 (240 gridpoints) while the gradient wind calculations further reduce it to 14 x 13 (182 gridpoints). The grid array has been made large enough so that truncation does not affect the Great Lakes region. Reliable sealevel pressure analyses and geostrophic wind analyses have been made while curvature analyses and gradient wind analyses have been produced that show discrepancies when compared with hand analyses or measured values.

The Analysis Method

For purposes of explanation, consider the pressure analysis for the area shown in Figure E-1. The SAT consists essentially of a method of successively correcting grid-point pressures using reported data. Smoothing is accomplished by the calculation of a mean correction for each scan as well as by the introduction of smoothing operations.

The First Guess Pressure Field

The SAT starts with a first guess grid-point pressure analysis. The first guess used for this analysis was obtained by advection of the pressure analysis of 6 hours earlier by 50% of the 500 mb wind. For the area under consideration, the Green Bay, Wisconsin, 500 mb wind was used in most cases. If no previous computer analysis existed, a hand analysis of the previous map was produced and advected for use as the first guess.

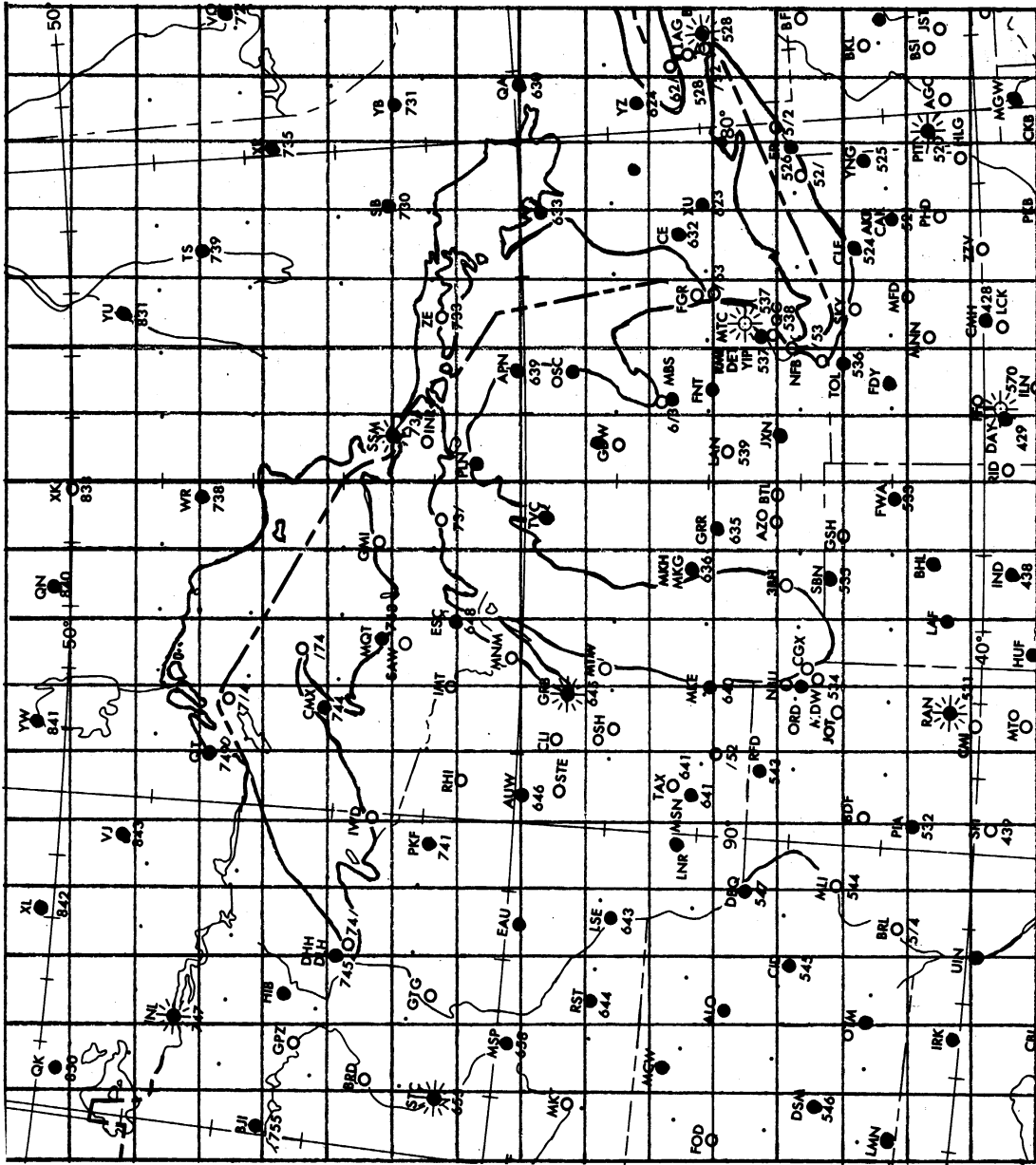


Figure E-1. The analysis grid and the locations of data sources for the Successive Approximation Technique.

The First Scan

For the first scan or iterative correction process, all pressure measurements within 4.75 grid lengths of each grid point were used to correct the grid point pressure. The amount of correction contributed by any measured station pressure is weighted inversely to its distance from the grid point. Specifically, the following procedures were followed for the first scan.

- a. All weather stations within a radius of 4.75 grid lengths of the grid point being considered were identified.
- b. For each of these stations the interpolated station pressure was calculated by bilinear interpolation from the first guess pressure field. The difference between the interpolated and measured station pressure is the error of the first guess field at the station location.

$$ER = P_{\text{measured}} - P_{\text{interpolated}}$$

- c. A weight function for each weather station within the 4.75 grid length radius of the grid point in question was calculated.

$$WT = \frac{N^2 - d^2}{N^2 + d^2}$$

where N = scanning radius

d = distance from grid point to station.

Note that the WT is unity for a station on a grid point and is zero for a station one scanning radius from the grid point. The weight was zero for all stations outside of the scanning radius.

- d. The correction applied to the grid point was:

$$\text{correction} = \frac{\sum WT * ER}{\sum \text{stations}}$$

where Σ stations = the total number of stations contributing to the correction. Thus the correction was a mean value of weighted errors.

Scans Two and Three

Scans two and three followed the same procedure as scan one except the scanning radius, N , was decreased to 3.60 and 2.25 grid lengths respectively. The results of each previous scan were used as the input pressure fields. By reducing the radius of influence, the measured data closer to each grid point more strongly influenced the correction for the grid point.

The First Smoothing

To suppress calculation instabilities, the grid point pressures were smoothed between scans three and four and after scan four. Interior grid points were smoothed by the following five point smoother. Where

$$\begin{array}{ccccc}
 & & +p_1 & & \\
 & & & & \\
 & +p_2 & +p_0 & +p_4 & \\
 & & & & \\
 & & +p_3 & & \\
 \\
 \text{Smoothed } p_0 & = & p_0 & + & \frac{1}{8} \nabla^2 p_0 \\
 \\
 & = & \frac{4 * p_0 + p_1 + p_2 + p_3 + p_4}{8}
 \end{array}$$

For perimeter grid points, the following smoothing was used:

$$\begin{array}{ccccc}
 & & & & +p_1 \\
 & & & & +p_0 \\
 & & & & +p_2 \\
 \\
 p_1 & p_0 & p_2 & & \\
 + & + & + & \text{or} & \\
 & & & &
 \end{array}$$

$$\text{Smoothed } p_0 = \frac{2 * p_0 + p_1 + p_2}{4}$$

The corner grid points were not smoothed.

The Fourth Scan

The technique of scan one was used for scan four with the scanning radius = 1.5 grid lengths and the correction given by:

$$\text{correction} = \frac{\sum WT * ER}{\sum WT}$$

The Second Smoothing

The second smoothing was done the same as the first and the resultant smoothed pressure values constituted the pressure analysis according to the successive approximation technique.

The Geostrophic Wind Field

The u and v components of the geostrophic wind at each grid point were calculated from standard meteorological equations in centered finite difference form.

$$u_0 = - \frac{1}{\rho f} \frac{p_1 - p_3}{y_1 - y_3}$$

$$v_0 = \frac{1}{\rho f} \frac{p_4 - p_2}{x_4 - x_2}$$

where f = the Coriolis parameter

ρ = the density

$$\begin{array}{ccccc}
 & & & & +p_1 \\
 & & & & \\
 +p_2 & & +p_0 & & +p_4 \\
 & & & & \\
 & & & & +p_3
 \end{array}$$

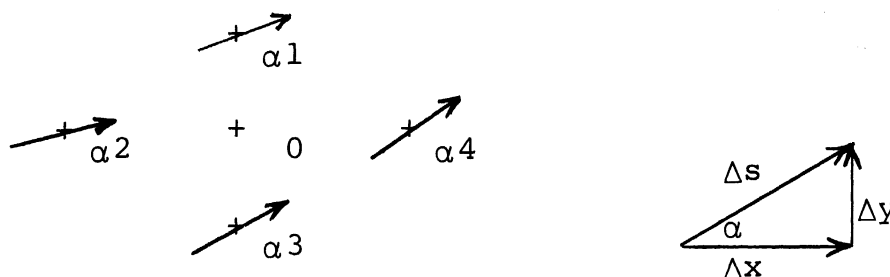
The magnitude and direction of the geostrophic wind relative to the grid were calculated from the following equation:

$$|V_{\text{geo}}| = \sqrt{u^2 + v^2}$$

Direction = $\beta = \arctan u/v$ where β = the meteorological definition of wind direction, i.e. the direction from which the wind is blowing.

The Radius of Curvature of the Wind Field

The curvature of the wind field is required in order to compute the gradient wind or the Bretschneider wind. The radius of curvature, R, was computed directly from the geostrophic wind direction by considering the change of wind direction between grid points.



$$K = \frac{1}{R} = \frac{d\alpha}{ds} = \frac{\partial \alpha}{\partial x} \frac{dx}{ds} + \frac{\partial \alpha}{\partial y} \frac{dy}{ds}$$

$$K_0 \approx \frac{\Delta \alpha}{\Delta x}_0 * \cos \alpha_0 + \frac{\Delta \alpha}{\Delta y}_0 \sin \alpha_0$$

$$= \frac{\alpha_4 - \alpha_2}{2L} * \cos \alpha_0 + \frac{\alpha_1 - \alpha_3}{2L} * \sin \alpha_0$$

where:

K = the curvature of the streamlines, which is a good approximation to the trajectory curvature

R = radius of curvature

α = angle of the wind vector, measured clockwise from the positive x axis

$\alpha = 3\pi/2 - \beta$ radians
 s = distance along a streamline
 L = grid spacing

The Gradient Wind Field

With the geostrophic wind and the radius of curvature computed for the grid points, the gradient wind was computed from standard meteorological equations.

$$V_g = -\frac{fR}{2} + \sqrt{\frac{f^2 R^2}{4} + fRV_{geo}} \quad \text{for cyclonic curvature}$$

$$V_g = \frac{fR}{2} - \sqrt{\frac{f^2 R^2}{4} - fRV_{geo}} \quad \text{for anticyclonic curvature}$$

The SAT pressure analysis described above and the geostrophic and gradient wind calculations were made from input pressure values at 114 weather stations. Bilinear interpolation provided pressure and wind at any location in the region. For evaluation of the technique, 47 winds at shoreline locations plus pressure and wind data from five ships per lake were entered into the computer but withheld from the analysis. The program compared these reports with the computed values and listed input values, computed values and the errors between them.

The output can be varied depending on use. One map output, a portion of which is shown in Figure E-2 lists the pressure, geostrophic wind, curvature and gradient wind at each interior grid point. In addition, it lists the input station pressures, the shoreline station winds, the ship weather reports, computed values of all parameters and errors. The overlake atmospheric stability, $T_{lake} - T_{air}$, is listed and averaged for each lake.

The input pressure can be listed as shown in Figure E-3 and the calculated gridpoint pressures as in Figure E-4. Contouring of the pressure field as shown by Figure E-5 is also possible but rather costly in time.

01	02	03	04	05	06	07	08	09	10	11	12	13	14	15	16	17	18
*	*	*	*	*	*	*	*	*	*	*	*	*	*	*	*	*	*
17*	58	68	73	75	78	80	82	83	86	92	101	108	112	114	115	117	116
16*	61	64	63	62	63	63	68	75	77	82	92	100	106	107	105	104	105
15*	58	53	44	41	45	46	52	62	68	75	84	92	99	102	100	96	96
14*	48	39	30	28	34	34	39	49	62	71	78	84	91	96	95	89	88
13*	35	23	15	17	26	27	33	43	56	67	74	79	83	87	86	83	84
12*	32	17	11	11	17	20	27	38	52	64	74	81	80	84	91	91	92
11*	36	25	19	15	9	9	21	36	52	68	81	86	87	90	100	105	106
10*	42	31	29	27	18	16	25	42	56	71	84	89	91	96	107	112	111
09*	57	44	43	44	42	38	43	56	66	78	89	95	98	104	113	116	119
08*	73	69	67	66	63	54	57	69	78	87	98	107	112	117	123	126	130
07*	81	88	87	83	74	63	67	79	89	97	107	116	122	127	134	138	143
06*	90	95	93	89	80	73	78	90	100	109	117	123	129	135	145	152	158
05*	103	102	100	97	90	85	89	102	112	119	124	129	136	144	156	164	171
04*	110	110	109	105	96	92	99	113	123	130	134	138	146	155	165	177	188
03*	112	115	115	111	108	107	112	123	135	143	148	152	158	165	176	189	200
02*	112	118	112	108	117	119	121	132	147	156	160	164	169	178	188	196	204
01*	108	117	114	113	120	126	131	143	157	166	167	169	176	185	192	199	206
*	*	*	*	*	*	*	*	*	*	*	*	*	*	*	*	*	*
01	02	03	04	05	06	07	08	09	10	11	12	13	14	15	16	17	18

Figure E-4. Gridpoint pressures as calculated by the Successive Approximation Technique.

01	02	03	04	05	06	07	08	09	10	11	12	13	14	15	16	17	18	
*	*	*	*	*	*	*	*	*	*	*	*	*	*	*	*	*	*	
5																		11
17*	*	666666	666666	888888	888888	888888	888888	888888	888888	00000000	00000000	00000000	00000000	00000000	00000000	00000000	00000000	* *17
16*	*	666666	666666	666666	666666	666666	666666	666666	888888	888888	888888	00000000	00000000	00000000	00000000	00000000	00000000	* *16
15*	*	444444	444444	444444	444444	444444	666666	666666	888888	888888	888888	888888	888888	888888	888888	888888	888888	* *15
14*	*	444444	222222	222222	222222	444444	444444	666666	888888	888888	888888	888888	888888	888888	888888	888888	888888	* *14
13*	*	2222	2222	2222	2222	4444	4444	6666	8888	8888	8888	8888	8888	8888	8888	8888	8888	* *13
12*	*	222	222	222	222	444	444	666	888	888	888	888	888	888	888	888	888	* *12
11*	*	2222	2222	000000	000000	222	222	444	666	888	888	888	888	888	00000000	00000000	00000000	* *11
10*	*	44	22222222	22222222	22222222	2222	2222	444	666	888	888	888	888	888	000000	00000000	00000000	* *10
09*	*	4444	44444444	44444444	44444444	4444	4444	6666	8888	8888	8888	8888	8888	8888	000000	00000000	2222	* *09
08*	*	66666666	66666666	66666666	66666666	6666	6666	8888	8888	8888	8888	8888	8888	8888	8888	8888	8888	* *08
07*	*	88888888	88888888	88888888	88888888	8888	8888	8888	8888	8888	8888	8888	8888	8888	8888	8888	8888	* *07
06*	*	888888	888888	888888	888888	8888	8888	8888	8888	8888	8888	8888	8888	8888	8888	8888	8888	* *06
05*	*	0000000000	0000000000	000000	000000	8888888888	8888888888	8888888888	8888888888	8888888888	8888888888	8888888888	8888888888	8888888888	8888888888	8888888888	8888888888	* *05
04*	*	00000000000000	00000000000000	00000000	00000000	8	0000	2222	2222	2222	2222	2222	2222	2222	2222	2222	2222	* *04
03*	*	0000000000000000	0000000000000000	0000000000000000	0000000000000000	2222	2222	2222	2222	2222	2222	2222	2222	2222	2222	2222	2222	* *03
02*	*	000	000	000	000	22222222	22222222	4444	4444	4444	4444	66666666	888888	888888	00000000	00000000	00000000	* *02
01*	*	000000000000000000	000000000000000000	000000000000000000	000000000000000000	4444	4444	4444	4444	4444	4444	4444	4444	4444	4444	4444	4444	* *01
10																		20

Figure E-5. Contours of the calculated pressure field.

Evaluation of the Successive Approximation Technique

Comparisons between measured ship pressures and computed ship pressures show the SAT does indeed analyze the pressure field. The geostrophic wind field appears to be smooth and regular and compares well with the measured winds. The radius of curvature field shows irregularities and inconsistencies that point out a need for further development. The gradient wind field is not a smooth field with reasonable values but is quite irregular and not an acceptable analysis. The poorness of this analysis is undoubtedly due to the poor radius of curvature input. It must be concluded, at this time, that the SAT produces good pressure and geostrophic wind analyses but the radius of curvature and gradient wind analyses are unreliable. For the development of a wave climatology, the SAT is feasible for the determination of geostrophic wind. Curvature, however, should be determined from measurements on hand analyzed charts until more consistent machine results can be obtained.

APPENDIX F

DERIVATION OF THE SIGNIFICANT WAVE
HEIGHT AS A FUNCTION OF THE STANDARD DEVIATION

APPENDIX F

Derivation of the Significant Wave Height
as a Function of the Standard Deviation

The height of the lake surface, $h(t)$, is a classical random variable and must be analyzed by the techniques of random data analysis. Bendat and Piersol (1966) define the mean square value, Ψ_h^2 , of random data to be:

$$\Psi_h^2 = \lim_{T \rightarrow \infty} \frac{1}{T} \int_0^T h^2(t) dt \quad (F-1)$$

and the variance to be:

$$\tau_h^2 = \lim_{T \rightarrow \infty} \frac{1}{T} \int_0^T [h(t) - \mu_h]^2 dt \quad (F-2)$$

where μ_h is the mean value of the lake level.

$$\mu_h = \lim_{T \rightarrow \infty} \frac{1}{T} \int_0^T x(t) dt \quad (F-3)$$

By a change of coordinates such that $h(t)$ is measured from the mean lake level, μ_h can be made zero over the time period 0 to T and

$$\Psi_h^2 = \tau_h^2 = \lim_{T \rightarrow \infty} \frac{1}{T} \int_0^T h^2(t) dt \quad (F-4)$$

This should be compared with Jacobs' (1965) equation (4) chapter 2.

$$E = 2 \lim_{T \rightarrow \infty} \frac{1}{T} \int_0^T h^2(t) dt \quad (F-5)$$

where E is the PNJ energy parameter.
From (F-4) and (F-5), we obtain:

$$\tau_h^2 = \frac{E}{2} \quad (F-6)$$

and the root mean square wave height (the positive square root of the variance)

$$\tau_h = \left(\frac{E}{2}\right)^{1/2} \quad \text{and} \quad E = 1.414 \tau_h \quad (\text{F-7})$$

Pierson, Neumann and James (1955) have stated that the significant wave height, $H_{1/3}$, can be determined from the E value of a sea state by:

$$H_{1/3} = 2.83 \quad E = 2.83 * 1.44 \tau_h \quad (\text{F-8})$$

or

$$H_{1/3} = 4 \tau_h \quad (\text{F-9})$$

The analog computer analysis used to compute τ_h removes the mean value μ_h from the data, so equation (F-9) can be used to determine $H_{1/3}$.

BIBLIOGRAPHY

- Arthur, R. S., 1947: Revised wave forecasting graphs and procedures. Wave Report No. 73, Scripps Institute of Oceanography, 14 pp.
- Bendat, J. S. and A. G. Piersol, 1966: Measurement and Analysis of Random Data. John Wiley and Sons, Inc., New York.
- Bellaire, F. R., 1965: The modification of warm air moving over cold water. Proceedings of the Eight Conference on Great Lakes Research, March 29-30, 1965, Ann Arbor, Michigan, pp. 249-256.
- Bretschneider, C. L., 1951: Revised wave forecasting curves and procedures. Technical Report No. HE-155047, Institute of Engineering Research, University of California, Berkeley, 28 pp. (Unpublished).
- _____, 1957: Revisions in wave forecasting: deep and shallow water. Proceedings VI th. Conference on Coastal Engineering, Chapter 3, pp. 30-67.
- _____, 1959: Wave variability and wave spectra for wind generated gravity waves. Beach Erosion Board, U.S. Army Corps of Engineers, Technical Memo. No. 118, pp. 192.
- _____, 1965: Generation of waves by wind. State of the Art, Report by National Engineering Science Company, Washington, D.C., 20036.
- Caldwell, J. M., 1963: Rapid spectrum of ocean wave trains. Proceedings of the International Association of Hydraulic Research Congress, Vol. 1, pp. 205, London.
- _____, and L. C. Williams, 1963: The Beach Erosion Board's Wave Spectrum Analyzer and its Purpose, Ocean Wave Spectra, Prentice Hall, pp. 259-266.
- Cressman, G. P., 1959: An operational objective analysis system. Monthly Weather Review, Vol. 87, No. 10, pp. 367-374.

- Elder, F. C., 1965: An investigation of atmospheric turbulent processes over water, report number two: data, 1963 and 1964. Contract Cwb-10714, University of Michigan Report 05982-1-f. pp. 71.
- Harris, D. L., 1967: The air-sea boundary layer. Paper presented at the Conference of the American Meteorological Society on Physical Processes in the Lower Atmosphere, March 20-22, 1967, Ann Arbor, Michigan.
- Jacobs, S. J., 1965: Wave hindcasts vs. recorded waves. Final Report 06768-1-f. Office of Research Administration, University of Michigan, Ann Arbor, Michigan.
- Kitaigorodski, S. A., 1961: Application of the theory of similarity to the analysis of wind-generated wave motion as a stochastic process. *IZV, Geophys. Ser.*, pp. 105-117.
- Lansing, L., 1965: Air mass modification by Lake Ontario during the April-November period. Proceedings of the Eighth Conference on Great Lakes Research, March 29-30, 1965, Ann Arbor, Michigan, pp. 257-261.
- Lonquet-Higgins, M. S., 1952: On the standard distribution of the heights of sea waves. Journal of Marine Research, Vol. XI, No. 3, pp. 345-366.
- Newmann, G., 1952: On ocean wave spectra and a new method of forecasting wind-generated sea. Beach Erosion Board, U.S. Army Corps of Engineers, Tech. Memo. No. 43, pp. 42
- Pierson, W. J. Jr., 1964: The interpretation of wave spectrums in terms of the wind profile instead of the wind measured at a constant height. Journal of Geophysical Research, Vol. 69, No. 24, pp. 5191-5203.
- _____, G. Newmann, and R. James, 1955: Practical methods for observing and forecasting ocean waves. H.O. Publ. 603, U.S. Navy Hydrographic Office.
- _____, and L. Moskowitz, 1964: A proposed spectral form for fully developed seas based on the similarity theory of S.A. Kitaigoradskii. Journal of Geophysical Research, Vol. 69, pp. 5181-5190.

Richards, T. L., H. Dragert and D. R. MacIntyre, 1966: Influence of atmospheric stability and over-water fetch on winds over the lower Great Lakes. Monthly Weather Review, Vol. 94, No. 1, pp. 448-453.

Strong, A. E., and F. R. Bellaire, 1965: The effect of air stability on wind and waves. Proceedings of the Eight Conference on Great Lakes Research, March 29-30, 1965, Ann Arbor, Michigan, pp. 283-289.

Sverdrup, H. U. and W. H. Munk, 1947: Wind, sea and swell: theory of relations for forecasting. Hydrographic Office Publ. No. 601. U.S. Department of the Navy, pp. 44.

U.S. Army Corps of Engineers, 1961: Shore protection, planning and design. Beach Erosion Board Technical Report No. 4 (BEB T.R. 4), Rev.



THE UNIVERSITY OF MICHIGAN

DATE DUE

8/29 5:55pm